
Learn from Your Mistakes: Self-Correcting Masked Diffusion Models

Anonymous Authors¹

Abstract

Masked diffusion models (MDMs) have emerged as a promising alternative to autoregressive models, enabling parallel token generation while achieving competitive performance. Despite these advantages, MDMs face a fundamental limitation: once tokens are unmasked, they remain fixed, leading to error accumulation and ultimately degrading sample quality. We address this by proposing a framework that trains a model to perform both unmasking and correction. By reusing outputs from the MDM denoising network as inputs for corrector training, we train a model to recover from potential mistakes. During generation we apply additional corrective refinement steps between unmasking ones in order to change decoded tokens and improve outputs. We name our training and sampling method *Progressive Self-Correction (ProSeCo)* for its unique ability to iteratively refine an entire sequence, including already generated tokens. We conduct extensive experimental validation across multiple conditional and unconditional tasks, demonstrating that *ProSeCo* yields better quality-efficiency trade-offs (up to $\sim 4x$ faster sampling) and enables inference-time compute scaling to further increase sample quality beyond standard MDMs (up to $\sim 1.2x$ improvement on benchmarks).

1. Introduction

Masked diffusion models (MDMs) (Lou et al., 2024; Ou et al., 2024; Sahoo et al., 2024a; Shi et al., 2024) have emerged as a powerful paradigm for discrete data generation and offer a compelling alternative to autoregressive (AR) models. By denoising via parallel unmasking, MDMs can achieve efficiency gains across various domains, and have

¹Anonymous Institution, Anonymous City, Anonymous Region, Anonymous Country. Correspondence to: Anonymous Author <anon.email@domain.com>.

Preliminary work. Under review by the International Conference on Machine Learning (ICML). Do not distribute.

even demonstrated competitive performance from the 8B scale (Nie et al., 2025) up to 100B. (Bie et al., 2025).

However, a fundamental limitation persists for MDMs: once a token is unmasked, it remains fixed for the duration of the generation process. Consequently, errors made during parallel decoding inevitably accumulate, leading to distributional drift and degraded sample quality. While recent work has begun to explore error correction for MDMs (Huang et al., 2025; Kim et al., 2025a; Lezama et al., 2023; Liu et al., 2026; Wang et al., 2025a; Zhao et al., 2024b), efficiently identifying which tokens require modification and altering them remains a significant challenge.

In this work, we address this limitation by proposing a principled framework that equips MDMs with the ability to both decode and correct. Our method trains a model to recover the clean signal from its own potentially mistaken outputs, enabling it to learn from and correct its own failures. We implement this training via a simple additional cross-entropy loss term added to standard MDM objectives. During inference, we leverage this capability by interleaving corrective steps in between standard unmasking steps, allowing the model to dynamically refine and “self-correct” outputs. The training and inference modifications we make to existing MDM algorithms are minimal, yet lead to marked gains. We name our approach *Progressive Self-Correction (ProSeCo)*, since our method has the ability to iteratively refine all positions in a sequence, including ones already unmasked.

On math and coding benchmarks, our method significantly improves standard fine-tuning of large MDMs, enabling $\sim 2-4x$ faster generation without quality degradation, and up to $\sim 1.2x$ increase in benchmark accuracy. For guided generation, we demonstrate that recovering from mistaken tokens improves the Pareto frontier of sample quality and property maximization. Finally, we also demonstrate that for unconditional generation, our method improves over MDMs and other proposed correctors in terms of generating fluent text without collapsing the diversity of generated outputs. Across all experiments we demonstrate that *ProSeCo* better trades-off quality and speed, and can also benefit from inference-time scaling to further increase sample quality.

In summary, our contributions are as follows: 1) We present a framework that jointly trains for decoding masked tokens and correcting mistakes. 2) We provide easy-to-implement

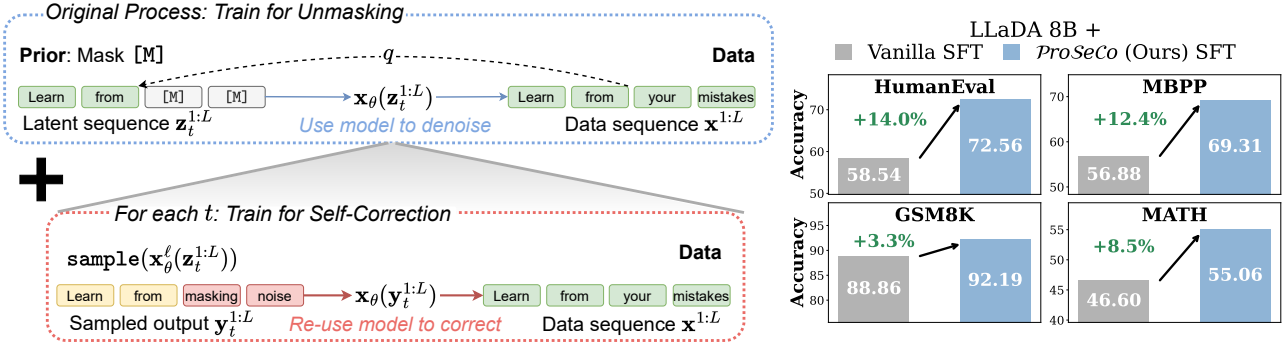


Figure 1. (Left) Training *ProSeCo*: The original process trains for generation via unmasking. For every timestep in the masking process, we also train for self-correction: undoing corruptions that arise from sampling from unmasking predictions. (Right) Using our method to supervised fine-tune (SFT) the 8B parameter LLaDA model (Nie et al., 2025) significantly outperforms vanilla masked diffusion SFT.

training and sampling algorithms that entail only minor additions to standard MDM. 3) We conduct comprehensive experiments demonstrating that *ProSeCo* outperforms quality-efficiency trade-offs of other methods and enables inference-time compute scaling to further improve quality.

2. Background

Discrete Diffusion Diffusion is a paradigm for generative modeling where a denoising process p_θ is trained to undo a pre-defined corruption process q (Sohl-Dickstein et al., 2015; Song & Ermon, 2019; Song et al., 2020). Starting from data $\mathbf{x} \sim q_{\text{data}}$, the corruption process produces latent variables $\mathbf{z}_t \sim q(\mathbf{z}_t | \mathbf{x})$ for $t \in [0, 1]$, which increasingly move further from the data and towards noise, as t increases.

Adapting diffusion models to discrete data requires a corruption process over the space of sequences of tokens with values in a finite vocabulary (Austin et al., 2021a). To denote this data, we let $\mathbf{x}, \mathbf{z}_t \in \mathcal{V}$, where $\mathcal{V} := \{0, 1\}^V \subset \Delta^V$, and Δ^V denotes the probability simplex over V categories. We use superscripts to denote the sequence dimension; for example, $\mathbf{x}^{1:L} \in \mathcal{V}^L$ represents a sequence of tokens $(\mathbf{x}^1, \dots, \mathbf{x}^L)$, where token $\mathbf{x}^\ell \in \mathcal{V}$, for $\ell \in \{1, \dots, L\}$.

Masked Diffusion Models For masked diffusion models (MDM; (Lou et al., 2024; Ou et al., 2024; Sahoo et al., 2024a; Shi et al., 2024)), the corruption process is characterized by marginals that interpolate between data and noise: $q(\mathbf{z}_t | \mathbf{x}) = \text{Cat}(\mathbf{z}_t; \alpha_t \mathbf{x} + (1 - \alpha_t) \mathbf{m})$, where \mathbf{m} denotes the one-hot vector for a special [M] token and $\alpha_t := \alpha(t) \in [0, 1]$ is a noise schedule that is monotonically decreasing in t . In MDM, the corruption process is defined to be ‘absorbing,’ meaning that once a token transitions to the masked state, it remains in this state.

Diffusion models are trained via a variational bound on the negative log-likelihood (NLL). This bound encourages the learned approximate posterior $p_\theta(\mathbf{z}_s | \mathbf{z}_t)$ to match the true one $q(\mathbf{z}_s | \mathbf{x}, \mathbf{z}_t)$, for $s < t$ (Sohl-Dickstein et al.,

2015). For MDMs, the true posteriors take the following form (Austin et al., 2021a; Sahoo et al., 2024a):

$$q(\mathbf{z}_s | \mathbf{x}, \mathbf{z}_t \neq \mathbf{m}) = \text{Cat}(\mathbf{z}_s; \mathbf{z}_t),$$

$$q(\mathbf{z}_s | \mathbf{x}, \mathbf{z}_t = \mathbf{m}) = \text{Cat}\left(\mathbf{z}_s; \frac{\alpha_s - \alpha_t}{1 - \alpha_t} \mathbf{x} + \frac{1 - \alpha_s}{1 - \alpha_t} \mathbf{m}\right). \quad (1)$$

A common parameterization for $p_\theta(\mathbf{z}_s | \mathbf{z}_t)$ replaces \mathbf{x} in (1) with the output of a neural network: $\mathbf{x}_\theta(\mathbf{z}_t) \in \Delta^V$. In the continuous-time limit, the objective for MDMs simplifies to (Ou et al., 2024; Sahoo et al., 2024b; Shi et al., 2024):

$$\mathcal{L}_\theta^{\text{MDM}} := \mathbb{E}_{q_{\text{data}}} \int_0^1 \mathbb{E}_{q_t} \sum_{\ell=1}^L \delta_{\mathbf{z}_t^\ell, \mathbf{m}} \frac{\dot{\alpha}_t}{1 - \alpha_t} \log \langle \mathbf{x}_\theta^\ell(\mathbf{z}_t^{1:L}), \mathbf{x}^\ell \rangle dt, \quad (2)$$

where $\dot{\alpha}_t$ denotes the time derivative of the noise schedule, $\delta_{\mathbf{a}, \mathbf{b}} := \delta(\mathbf{a}, \mathbf{b})$ is the Kronecker delta function that evaluates to 1 if $\mathbf{a} = \mathbf{b}$, $\mathbb{E}_{q_{\text{data}}}$ refers to the expectation over drawing data samples $\mathbf{x}^{1:L} \sim q_{\text{data}}$, and \mathbb{E}_{q_t} is the expectation over drawing noisy latents from the forward marginals $\mathbf{z}_t^{1:L} \sim q(\mathbf{z}_t^{1:L} | \mathbf{x}^{1:L})$. We optimize this objective via stochastic gradient descent using Monte Carlo samples for the expectations and $t \sim \mathcal{U}[0, 1]$ to approximate the integral.

A key drawback of this paradigm is that the denoising network \mathbf{x}_θ does not learn to modify unmasked inputs $\mathbf{z}_t \neq \mathbf{m}$. Without the ability to correct mistakes, during generation, errors propagate and accumulate over time, causing the sampling trajectory to deviate from the true data distribution.

3. Self-Correcting Masked Diffusion Models

In this work, we aim to equip MDMs with the ability to alter previously decoded tokens. Our approach is to have a single model that can act in two ‘modes’: when inputs contain masked tokens, the model’s role is to unmask; when inputs contain all non-mask tokens, the model operates in ‘corrector’ mode and can update already generated positions.

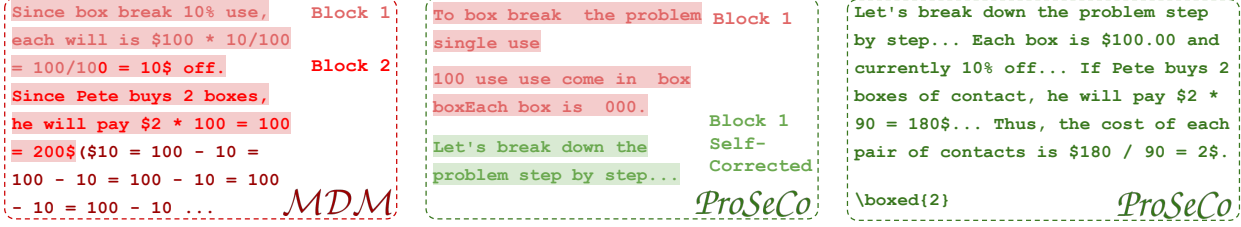


Figure 2. Illustrative example demonstrating the benefits of self-correction. (Left) For standard MDM, during parallel unmasking, errors occur. Mistakes accumulate and lead to sample collapse. (Middle) For *ProSeCo*, a short correction loop steers generation ‘back on track.’ (Right) *ProSeCo* can thus produce a final high quality output even with parallel generation.

Below, we present an augmented objective that trains models to jointly unmask and correct mistaken unmasked tokens. Our key insight is that during generation, \mathbf{x}_θ produces unmasked tokens at each position, some of which align with the true data distribution and some of which potentially contain errors or distributional misalignment. A subset of these tokens are then carried into the next round of iterative refinement. We can interpret outputs of \mathbf{x}_θ as corrupted sequences from the data distribution, where certain tokens have been replaced by incorrect ones sampled from \mathbf{x}_θ . This perspective motivates our formulation of model-generated sequences serving as inputs for a corrector model.

In Section 3.1, we introduce a straightforward corrector loss that we add to the MDM objective from (2), and we detail a training algorithm to efficiently and jointly train a model to unmask and correct decoding errors. Finally, in Section 4, we provide a sampling algorithm that leverages these abilities to further improve sample quality by interleaving error correction predictions and unmasking steps. Owing to this enhanced ability to iteratively refine any part of the sequence, including already decoded tokens, we dub our method *Progressive Self-Correction (ProSeCo)*.

3.1. Self-Correcting Objective

Our approach is to train a corrector to minimize error between outputs from the denoiser and clean data. By tying weights of the corrector and denoiser networks, we turn this formulation into an augmented MDM variational objective with an auxiliary error correction loss.

More precisely, let $\pi : \Delta^V \rightarrow \mathcal{V}$ generate samples from the MDM denoiser model. Then we define the input to our corrector as $\mathbf{y}_t^{1:L} := (\pi \circ \mathbf{x}_\theta^1(\mathbf{z}_t^{1:L}), \dots, \pi \circ \mathbf{x}_\theta^L(\mathbf{z}_t^{1:L}))$. We present the following objective for training a corrector alongside the standard MDM denoiser:

$$\mathcal{L}_{\phi, \theta}^{\text{MDM}} := \mathbb{E}_{q_{\text{data}}} \int_0^1 \mathbb{E}_{q_t} \sum_{\ell=1}^L \left[\underbrace{\lambda_t \log \langle \mathbf{x}_\theta^\ell(\mathbf{y}_t^{1:L}), \mathbf{x}^\ell \rangle}_{\mathcal{L}^C} + \underbrace{\frac{\dot{\alpha}_t}{1 - \alpha_t} \delta_{\mathbf{z}_t^\ell, m} \log \langle \mathbf{x}_\theta^\ell(\mathbf{z}_t^{1:L}), \mathbf{x}^\ell \rangle}_{\mathcal{L}^{\text{MDM}}} dt \right], \quad (3)$$

where ϕ denote the parameters of a corrector model $\mathbf{x}_\theta^\ell(\mathbf{y}_t^{1:L}) \in \Delta^V$. The standard MDM loss in the second term ensures that we train a useful denoiser \mathbf{x}_θ that generates meaningful candidates for \mathbf{x}_θ to correct. In addition to the MDM objective, we add a correction loss \mathcal{L}^C to every term in the integrand. This auxiliary loss amounts to a simple cross-entropy (CE) term, which encourages the model to identify and correct mistakes from the original denoising network. The weighting $\lambda_t := \lambda(t) < 0$ lets us control the relative weight between the correction and diffusion losses.

Algorithm 1 *ProSeCo* Training

Differences from standard MDM training highlighted in **brown**.
Input: Training data \mathcal{D} , model \mathbf{x}_θ with parameters θ , corruption process q , noise schedule α_t .

- 1: **repeat**
- 2: Sample $\mathbf{x}^{1:L}$ i.i.d. from \mathcal{D}
- 3: Sample $t \sim \mathcal{U}[0, 1]$
- 4: Compute $\alpha_t, \dot{\alpha}_t$
- 5: Sample $\mathbf{z}_t^{1:L} \sim q(\mathbf{z}_t^{1:L} | \mathbf{x})$
- 6: Compute $\mathbf{x}_\theta(\mathbf{z}_t^{1:L})$
- 7: $\mathcal{L}_\theta^{\text{MDM}} \leftarrow \frac{\dot{\alpha}_t}{1 - \alpha_t} \sum_{\ell=1}^L \delta_{\mathbf{z}_t^\ell, m} \log \langle \mathbf{x}_\theta^\ell(\mathbf{z}_t^{1:L}), \mathbf{x}^\ell \rangle$
- 8: $\mathbf{y}_t^\ell \leftarrow \text{sg}(\text{one_hot}(\arg \max_i \mathbf{x}_\theta^\ell(\mathbf{z}_t)_i)), \forall \ell$
- 9: Compute $\mathbf{x}_\theta(\mathbf{y}_t^{1:L})$
- 10: $\mathcal{L}_\theta^{\text{SC}} \leftarrow \frac{\dot{\alpha}_t}{1 - \alpha_t} \sum_{\ell=1}^L \log \langle \mathbf{x}_\theta^\ell(\mathbf{y}_t^{1:L}), \mathbf{x}^\ell \rangle$
- 11: Perform gradient descent step on $\mathcal{L}_\theta^{\text{MDM}} + \mathcal{L}_\theta^{\text{SC}}$
- 12: **until** converged
- 13: **Return** θ

3.2. *ProSeCo* Design Decisions

Tying Corrector and Denoiser Weights In order to have a unified model that can both decode and correct, we elect to tie the weights $\phi = \theta$. This decision has the added benefit of eliminating memory overhead for training a separate corrector model. The error correction term in (3) thus becomes a self-correcting one: $\mathcal{L}^C \rightarrow \mathcal{L}^{\text{SC}}$

Selecting Transformation π To simplify optimization, we use $\arg \max$ sampling from $\mathbf{x}_\theta(\mathbf{z}_t^{1:L})$. This decision aligns with how state-of-the-art MDMs, such as LLaDA (Nie et al., 2025), are used in practice. Namely, during generation, at every iteration, each masked position from the output of \mathbf{x}_θ is decoded greedily. Then using some algorithm or heuristic,

we determine which positions to retain for the next round and which to keep masked.

Setting Corrector Loss Weight λ_t We found empirically that reusing the same factor from MDM was a performant strategy, i.e., $\lambda_t = \dot{\alpha}_t / (1 - \alpha_t)$. In addition to balancing both terms in our objective, this weighting scheme is justified intuitively. Specifically, in MDM, the weight $\dot{\alpha}_t / (1 - \alpha_t)$ discounts samples that are more heavily noised. For example, for the commonly used linear schedule $\alpha_t = 1 - t$, this term amounts to dividing by the expected proportion of masked tokens in a sequence, i.e., we discount the ‘harder’, more heavily masked sequences. For training the corrector model, it is reasonable to apply a similar rationale: sequences with heavy masking which are harder to denoise will also be harder to correct and should therefore be down-weighted.

Combining the above, yields our objective for effective joint denoising and self-correction training:

$$\mathcal{L}_\theta^{SCMDM} := \mathbb{E}_{q_{\text{data}}} \int_0^1 \mathbb{E}_{q_t} \frac{\dot{\alpha}_t}{1 - \alpha_t} \sum_{\ell=1}^L \left[\underbrace{\log \langle \mathbf{x}_\theta^\ell(\mathbf{y}_t^{1:L}), \mathbf{x}^\ell \rangle}_{\mathcal{L}^{SC}} + \underbrace{\delta_{\mathbf{z}_t^\ell, \mathbf{m}} \log \langle \mathbf{x}_\theta^\ell(\mathbf{z}_t^{1:L}), \mathbf{x}^\ell \rangle}_{\mathcal{L}^{MDM}} dt \right], \quad (4)$$

3.2.1. TRAINING WITH THE $SCMDM$ OBJECTIVE

In Algorithm 1, we present training for *ProSeCo*, which requires only minor modification to the standard MDM training. Specifically, in addition to the MDM forward pass used for (2), we sample from \mathbf{x}_θ , perform a second forward pass, and incorporate the corrector loss. A final modification to (4) is to wrap the denoiser model’s outputs in the stop-gradient operation $\text{sg}(\cdot)$ prior to forming the corrector input, which ensures training stability.

3.3. Theoretical Motivation

The corrector loss term in (3) can also be derived via the lens of learned predictor-corrector samplers for discrete diffusion models (Lezama et al., 2023; Zhao et al., 2024b). Specifically, deviations during sampling can be cast as a mismatch between marginals, that is $p_\theta(\mathbf{z}_t) \neq q(\mathbf{z}_t)$. If we apply the following Monte Carlo Markov Chain (MCMC) with a learned model p_ϕ :

$$\begin{aligned} \mathbf{y}_t^{1:L} &\sim p_\theta(\mathbf{y}_t^{1:L} | \mathbf{z}_t^{1:L}), \\ \hat{\mathbf{x}}^{1:L} &\sim p_\phi(\hat{\mathbf{x}}^{1:L} | \mathbf{y}_t^{1:L}), \\ \hat{\mathbf{z}}_t^{1:L} &\sim q(\hat{\mathbf{z}}_t^{1:L} | \hat{\mathbf{x}}^{1:L}), \end{aligned} \quad (5)$$

then the following condition ensures that the limiting distribution of transition kernels defined by (5) is $q(\mathbf{z}_t)$: $p_\phi(\mathbf{x}^{1:L} | \mathbf{y}_t^{1:L}) \propto p_\theta(\mathbf{y}_t^{1:L} | \mathbf{z}_t^{1:L}) q_{\text{data}}(\mathbf{x}^{1:L})$. Optimizing

Algorithm 2 *ProSeCo* Sampling

```

# Differences from standard MDM sampling
highlighted in brown.
Input: Model  $\mathbf{x}_\theta$ , length  $L$ , unmasking steps  $T$ , schedule  $\alpha_t$ ,
per step self-correction budget  $S$ , corrector frequency  $\omega$ .
1: Initialize  $\mathbf{z}_{t(T)}^{1:L} \leftarrow \mathbf{m}^{1:L}$ 
2: for  $i = T$  to 1 do
3:   logits  $\leftarrow \mathbf{x}_\theta(\mathbf{z}_t^{1:L})$ 
4:   if  $(T - i + 1) \bmod \omega == 0$  then
5:      $\mathbf{z}_t^{1:L}, \text{logits} \leftarrow \text{corrector}(\mathbf{x}_\theta, S, \mathbf{z}_t^{1:L}, \text{logits})$ 
// Algorithm 3
6:   end if
7:    $\mathbf{z}_{t(i-1)}^{1:L} \leftarrow \text{sample\_posterior}(\text{logits}, \mathbf{z}_t^{1:L}, \alpha_{t(i)})$ 
8: end for
9: Return  $\text{sample}(\mathbf{x}_\theta(\mathbf{z}_{t(0)}^{1:L}))$ 

```

Algorithm 3 *ProSeCo* Inner corrector loop

```

Input: Model  $\mathbf{x}_\theta$ , self-correction budget (per step)  $S$ , latent
sequence  $\mathbf{z}_t^{1:L}$ , denoising output logits
1: Initialize  $\mathbf{y}_t^\ell \leftarrow \text{one\_hot}(\arg \max_i \text{logits}_i), \forall \ell$ 
2: for  $S$  steps do
3:   corrector_logits  $\leftarrow \mathbf{x}_\theta(\mathbf{y}_t^{1:L})$ 
4:    $\mathbf{y}_t^{1:L} \leftarrow \text{sample}(\text{corrector\_logits})$ 
5: end for
# Correct unmasked positions in  $\mathbf{z}_t^{1:L}$ 
6:  $\mathbf{z}_t^\ell \leftarrow \mathbf{y}_t^\ell, \forall \mathbf{z}_t^\ell \neq \mathbf{m}$ 
7: Return  $\mathbf{z}_t^{1:L}, \text{corrector\_logits}$ 

```

ϕ so that this desired proportionality holds yields a loss term equivalent to that of \mathcal{L}^C (see Appendix A for full details).

4. Sampling with *ProSeCo*

In Algorithm 2, we present sampling for *ProSeCo*. Having a model that can jointly decode and correct allows us to interleave unmasking and correction steps. The goal of corrector iterations is two-fold: they should 1) potentially update already decoded positions in $\mathbf{z}_t^{1:L}$ and 2) provide improved predictions to be used for sampling in the unmasking posterior. To control the computation budget allocated to self-correction, we allow users to specify hyperparameters that determines how often a self-correcting loop is executed, ω , and the number of steps per loop, S .

In Algorithm 3, we present the self-correction procedure. We convert $\mathbf{x}_\theta(\mathbf{z}_t^{1:L})$ into a corrector input via $\arg \max$ sampling at every position. Within each correcting iteration, we use a `sample` method, e.g., greedy-max decoding, to generate the next corrector input sequence from the corrector model outputs. After the inner loop completes, unmasked positions $\mathbf{z}_t^\ell \neq \mathbf{m}$ are replaced with corresponding positions in the corrector sequence, which represents the remediation of already decoded tokens.

When operating as a strictly ‘unmasking’ model, an iteration of inference loop is identical to that in standard MDMs: input consists of a partially masked sequence

$\mathbf{z}_t^{1:L}$, it outputs predictions $\mathbf{x}_\theta^\ell(\mathbf{z}_t^{1:L})$ at every position ℓ , and we decide some tokens to unmask via a call to a `sample_posterior` protocol, which returns a sequence with fewer masked tokens. For example, we can use *ancestral sampling* (Sahoo et al., 2024b), where we replace \mathbf{x} with \mathbf{x}_θ in (1) and sample accordingly, the *confidence-based* approach proposed in Nie et al. (2025), where proposal tokens are selected greedily from $\mathbf{x}_\theta(\mathbf{z}_t^{1:L})$ and those with top- k confidence are retained for the next iteration, or one of other more recently proposed methods (Ben-Hamu et al., 2025; Kim et al., 2025b;c). If correction has been applied, instead of $\mathbf{x}_\theta(\mathbf{z}_t^{1:L})$, we use the corrector model’s last output for the `sample_posterior` routine, as the corrector model logits represent better informed predictions.

5. Experiments

We evaluate *ProSeCo* across a diverse set of tasks and for both conditional and unconditional generation. We consistently demonstrate that our model better scales the quality-efficiency frontier, and enables even further improvements via inference-compute scaling.

5.1. Math & Code Benchmarks

Setup To evaluate *ProSeCo* on large MDMs, we perform supervised fine-tuning (SFT) of the LLaDA-Base 8B model (Nie et al., 2025) using our training Algorithm 1. Specifically, we fine-tuned for $\sim 400\text{B}$ tokens on a modified version of the Llama-Nemotron-Post-Training dataset (Bercovich et al., 2026). In this variant, the target outputs for each prompt were generated using GPT-OSS (OpenAI, 2025). (see Appendix C.1 for full details). We then evaluate on downstream benchmarks for code: HumanEval (Chen et al., 2021) and MBPP (Austin et al., 2021b), and math: GSM8K (Cobbe et al., 2021) and MATH (Hendrycks et al., 2021). In addition to reporting metrics for open-sourced large AR and MDM models (with and without corrector mechanisms), for a direct comparison, we apply the SFT recipe using the standard MDM objective to LLaDA-Base.

Note that for all LLaDA-based models we apply the semi-AR sampling algorithm (Arriola et al., 2025) adopted by Nie et al. (2025), where the full generation sequence L is broken into blocks of size B and unmasking decoding is applied block-by-block from left-to-right (see Appendix B).

Main Results Table 1 represents our main results. The key finding is that for every benchmark, *ProSeCo* outperforms all diffusion baselines, including those coupled with other corrector mechanisms, and *ProSeCo* beats a comparably-sized instruction fine-tuned AR model (Llama3.1; (Grattafiori et al., 2024)). Moreover, our baseline SFT model (fourth row from the bottom) represents a strong watermark, significantly improving over the LLaDA-Base and even sur-

passing / matching the LLaDA instruction fine-tuned model. Nevertheless, SFT using *ProSeCo* outperforms this strong baseline. Notably, even before applying the *ProSeCo* sampling procedure from Algorithm 2, the model trained with the *ProSeCo* objective outperforms one trained with the standard MDM loss.

Analyzing the Quality-Efficiency Trade-off In Figure 3, we present an analysis of the quality-efficiency trade-offs for *ProSeCo*. Results further to the north-west corner are desirable as they indicate better performance with a smaller number of function evaluations (NFEs).

In standard MDM, the only lever for controlling this trade-off is number of inference steps used for unmasking, or in other words the number of token positions generated in parallel at each decoding step. For *ProSeCo*, we can also control the compute via the frequency of corrector loops and number of iterative refinement steps per loop.

For each benchmark, we find that *ProSeCo* can outperform the highest accuracy baseline configuration, i.e., generating one token in each iteration; depicted as the gray dot. As depicted by the green star marker labeled as “Fast,” we can strictly improve baseline accuracy with reduced NFEs by increasing the decoding parallelism (4 - 8 tokens) per unmasking step. To compensate for this, we apply corrector loops every 2 and use up to 4 NFEs per corrector loop. Replacing unmasking steps with correcting ones, leads $\sim 2\text{-}4\text{x}$ speed-ups relative to LLaDA decoding, while maintaining accuracy. *ProSeCo* also enables configurations that can moderately increase compute while delivering significant accuracy improvements, as depicted by the orange star marker labeled as “Balanced” (for best trade-off; see Appendix C.1 for details on how this point was selected). Finally, *ProSeCo* supports even further scaling of test-time compute to attain our highest performing results depicted in the blue star markers labeled as “Max.”

Pareto Frontier for Parallel Decoding and Quality Additionally, in Figure 4, we demonstrate that for standard MDMs, increasing the level of parallel decoding significantly degrades sample quality. In contrast, *ProSeCo* models can recover from the mistakes introduced during generation and better scale the parallel decoding-quality Pareto frontier.

Ablation: Selecting Corrector Budget Finally, in Appendix D.2 Figure 7, we explore performance of various configurations of our sampling hyperparameters to provide guidance on allocating the corrector budget, as determined by frequency (ω) of and number of steps (S) per loop. The key takeaway, is that our model is highly robust to the choice of these hyperparameters, beating the baseline accuracy at each token parallelism level regardless of choice of ω and S . Additionally for fast sampling regimes (tokens/step $\in \{4, 8\}$), we find that with more frequent corrector loops, we can

Table 1. Pass@1 on code and math benchmarks. ‘Corrector Sampling’ \times / \checkmark symbol indicates whether a correction algorithm was applied. \dagger indicates values taken from Huang et al. (2025). Other "Prior work" values obtained via evaluation with open-sourced weights.

			Code		Math	
		Corrector Sampling	HumanEval	MBPP	GSM8K	MATH
<i>Off-the-Shelf 8B Models</i>						
	Llama3.1-Instruct (Grattafiori et al., 2024)	\times	63.41	70.90	81.05	47.38
	LLaDA-Base (Nie et al., 2025)	\times	34.15	37.20	46.78	17.04
<i>Prior Work</i>	LLaDA-Instruct (Nie et al., 2025)	\times	45.73	47.09	83.40	43.14
	+ ReMDM (Wang et al., 2025a)	\checkmark	43.90	45.50	83.93	43.76
	LLaDA1.5 (Zhu et al., 2025)	\times	45.12	46.83	84.00	42.54
	ReMeDi-Instruct \dagger (Huang et al., 2025)	\checkmark	71.30	57.80	86.30	51.40
<i>Our SFT with LLaDA-Base 8B Model</i>						
<i>Baseline</i>	Vanilla SFT	\times	58.54	56.88	88.86	46.60
	+ ReMDM (Wang et al., 2025a)	\checkmark	56.10	50.00	88.48	46.22
<i>Ours</i>	<i>ProSeCo</i> SFT	\times	69.51	57.41	91.36	51.98
	+ <i>ProSeCo</i> Max Sampling	\checkmark	72.56	69.31	92.19	55.06

overcome the drop in quality from parallel decoding and even match or beat the baseline performance achieved with tokens/step = 1 with significant speed-up.

Ablation: Standard MDM + Self-Correction We apply self-correction sampling, Algorithms 2 and 3, to a vanilla SFT model. Table 6 (Appendix D.4), shows that standard MDM fails to correct errors, underscoring the core motivation of our work: the MDMs never learns to change already unmasked tokens so its output at unmasked positions is generally uninformative and does not lead to error correction.

5.2. Guided Molecule Design

In the context of guided generation, often when guidance strength is increased, model samples collapse. Our hypothesis is that *ProSeCo* can recover from these errors, thereby improving the guided generation trade-off of maximizing a property of interest while producing a diverse set of samples.

Setup We follow the experimental setup from Schiff et al. (2024) (see Appendix C.2 for more details). Specifically, we train models on string representations of molecules known as SMILES (Weininger, 1988) from the QM9 dataset (Ramakrishnan et al., 2014; Ruddigkeit et al., 2012). We then apply the discrete classifier-free-guidance (CFG) algorithm from Schiff et al. (2024) with varying unmasking budgets T and guidance strength γ . We measure the number of generated sequences that are valid (can be parsed by RDKit library (Landrum et al., 2013)), unique, and novel (do not appear in the QM9 dataset) as the metric for diverse, high quality samples, and for the novel sequences, we compute the mean property value as the metric for property maximization. We perform this experiment for two properties: ring count and drug-likeness (QED; (Bickerton et al., 2012)). We compare *ProSeCo* to an AR model, a diffusion model trained with uniform categorical noise (UDLM; (Schiff et al., 2024)), and a standard masked diffusion model (MDLM; (Sahoo

et al., 2024a)). We also compare to the three remasking strategies ReMDM (Wang et al., 2025a), ReMeDi (Huang et al., 2025), and GStar (Meshchaninov et al., 2025).

Results In Figure 5, we present the guidance results. Points further north-east are preferable, as they represent property maximization without sacrificing sample diversity and quality. For both properties of interest, *ProSeCo* pushes the Pareto frontier in the desired direction. This is particularly stark for experiments where we maximize the ring count property (left hand side of Figure 5).

Ablation on Choice of λ_t We ablate the effect of our choice of λ_t by repeating the guidance experiment for the ring count property with fixed $\lambda \in \{0.1, 1, 10\}$ and a time-varying weighted $\lambda_t \in \{0.1 \cdot \frac{\alpha_t}{(1-\alpha_t)}, 1 \cdot \frac{\alpha_t}{(1-\alpha_t)}, 10 \cdot \frac{\alpha_t}{(1-\alpha_t)}\}$. We report results in Figure 8 (Appendix D.5), where we find that our design choice of including $\frac{\alpha_t}{(1-\alpha_t)}$ in the corrector loss improves performance and that our model is robust to different scaling factors applied to this weighting scheme.

5.3. Unconditional Text Generation

Setup We train *ProSeCo* from scratch on the OpenWebText (OWT; (Gokaslan & Cohen, 2019)) dataset for 1M steps (Sahoo et al., 2024a) (see Appendix C.3 for details). We then generate 5000 samples consisting of $L = 1024$ tokens, for varying sampling budgets T . We compute MAUVE (Pillutla et al., 2021) and report the perplexity under the GPT2-Large model (Radford et al., 2019), to also measure quality, and average sequence entropy, to reflect diversity (Zheng et al., 2024). We compare against an AR model and MDLM (Sahoo et al., 2024a) without and with correctors: ReMDM (Wang et al., 2025a) and PRISM (Kim et al., 2025a). We also compare to the hybrid mask and uniform noise model GIDD (von Rütte et al., 2025).

For *ProSeCo*, we apply a 3 corrector steps after each un-

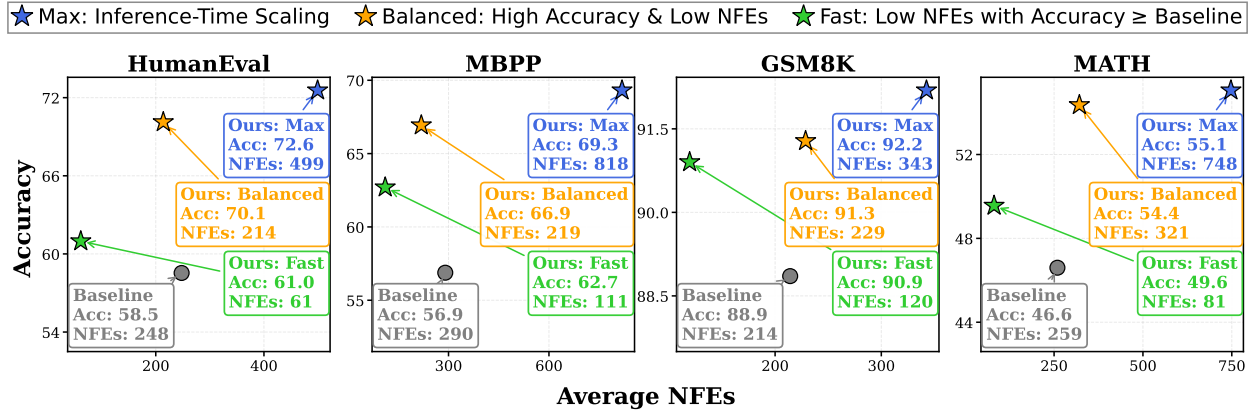


Figure 3. Quality-efficiency trade-offs. Standard MDMs (Baseline; gray dot) attain best performance decoding one token per step. *ProSeCo* can vary number of corrector steps and attain comparable performance more efficiently (Ours: Fast; green star), achieve better quality for modest increase in cost (Ours: Balanced; orange star), or maximize quality by further scaling compute (Ours: Max; blue star).

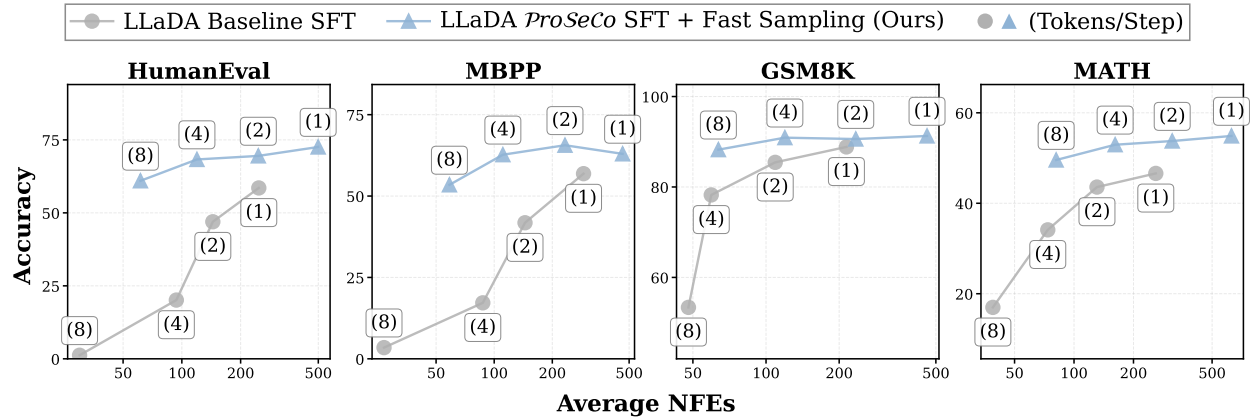


Figure 4. Pareto frontier of parallel decoding and quality. When decoding in parallel (i.e., fewer unmasking steps on x -axis), quality deteriorates. Applying a modest number of corrector steps, allows *ProSeCo* models to recover from these errors and extend this frontier.

masking step. For parity with the compute budget of other methods, we reduce the number of unmasking steps by a factor of 4 per sampling budget T . For this experiment, we use slightly modified training and sampling (Appendix C.3).

Results In Table 2, we see that across budgets, *ProSeCo* either significantly outperforms or matches baseline methods. Notably, even with just 256 steps, *ProSeCo* attains comparable sample quality to using PRISM with 2x or ReMDM with 4x the inference budget.

6. Related Works

Discrete Diffusion The seminal work of D3PM (Austin et al., 2021a) laid the foundation for adapting diffusion to discrete data. Some works extended this paradigm via the formalism of continuous-time Markov chains (Campbell et al., 2022; Lou et al., 2024). However, our method is more in line with the continuous-time extensions of the variational inference perspective (Ou et al., 2024; Sahoo et al., 2024b;

Shi et al., 2024). Previous efforts in this vein have relied on categorical uniform noise corruptions (Schiff et al., 2024; von Rütte et al., 2025) to alleviate the locked-in decoded tokens limitation of MDMs. Recently LLaDA 2.1 (Bie et al., 2026) scaled up the GIDD framework to 16B-100B parameters by fine-tuning with mixed mask and uniform noise. In contrast, our work which uses the model’s own unmasking output to train for correction, more closely aligns training and inference distributions, since during generation mistakes will not resemble uniform noise, but rather will come from the model’s own outputs. Our approach thus uses a more ‘informed’ noise relative to the mask-uniform hybrid approach.

Self-conditioning & Step Unrolling In self-conditioning (Chen et al., 2022; Dieleman et al., 2022), model’s prediction of clean data from one step inform future predictions. In prior works, predictions are simply provided as an auxiliary input, we use predictions to train self-correction and refine outputs during generation. Also related is training

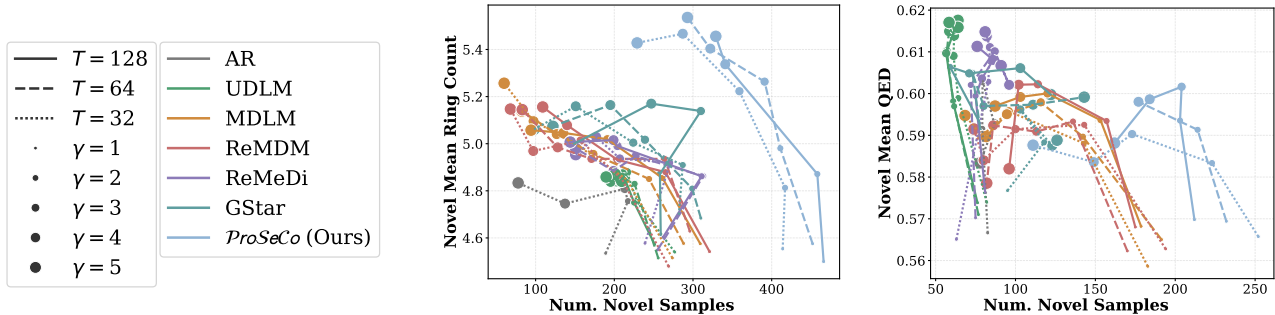


Figure 5. *ProSeCo* better navigates the novelty-property maximization Pareto frontier. Novel samples (x -axis) vs. mean property value of novel samples (y -axis) for classifier-free guidance (Schiff et al., 2024), with varying unmasking steps T (line style) and guidance strength γ (marker size). (Left) Maximizing the ring count property. (Right) Maximizing the drug likeness (QED) property.

Table 2. Sample quality for models trained on OpenWebText. [†] Values reported in Kim et al. (2025a). [§] Values reported in Wang et al. (2025a). * Open-sourced weights; sequence length reduced to 512 to match the model trained in von Rütte et al. (2025).

	MAUVE (\uparrow)				Gen. PPL (\downarrow)				Entropy (\uparrow)				
Data	1.00				14.8				5.44				
AR ($T = 1024$) [§]	0.76				12.1				5.22				
	$T =$	128	256	512	1024	128	256	512	1024	128	256	512	1024
MDLM [§] (Sahoo et al., 2024a)		0.015	0.023	0.031	0.042	61.5	55.8	53.0	51.3	5.52	5.49	5.48	5.46
ReMDM [§] (Wang et al., 2025a)		0.057	0.216	0.350	0.403	42.5	30.5	21.1	28.6	5.43	5.34	5.21	5.38
PRISM [†] (Kim et al., 2025a)		0.118	0.294	0.423	0.527	21.5	18.0	16.4	15.3	5.18	5.15	5.12	5.10
GIDD* (von Rütte et al., 2025)		0.268	0.284	0.334	0.356	95.1	80.5	76.9	76.1	5.00	4.94	4.94	4.94
<i>ProSeCo</i> (Ours)		0.295	0.557	0.597	0.604	23.1	16.5	13.2	10.9	5.45	5.39	5.29	5.22

on unrolled predictions from the denoising trajectory (Savinov et al., 2021). In this framework the model is trained on its own outputs of less noisy latent sequences, thereby more closely simulating the distribution seen during generation. Our method instead uses predictions of clean data, not unrolled trajectories of partially masked sequences.

Corrector Methods Several works used a predictor-corrector framework to improve sample quality, where, following an unmasking predictor step, a corrector step is applied to remask decoded positions (Campbell et al., 2022; Gat et al., 2024; Peng et al., 2025; Wang et al., 2025a). In contrast to these training free methods, other works propose to train an additional head to predict incorrect positions that should be remasked (Huang et al., 2025; Kim et al., 2025a; Lezama et al., 2023; Liu et al., 2026; Meshchaninov et al., 2025). More related to our work is Zhao et al. (2024b), which predicts corrections to already decoded tokens. However this method relies on a distinct Hollow Transformer backbone (Sun et al., 2022). This severely limits its application to fine-tuning of MDMs, e.g., LLaDA, pre-trained with the standard Transformer backbones.

7. Discussion & Conclusion

In this work, we presented a framework for jointly training a diffusion model to unmask and self-correct. We en-

able and take advantage of this new ability via minimal and straightforward modifications to standard MDM training and sampling algorithms. Evaluating on conditional and unconditional generation, across various model sizes, we demonstrated that our method consistently outperforms vanilla MDMs and alternative corrector methods both in terms of speed-quality tradeoffs and in the ability to further scale inference-time compute for improved generation.

Limitations The key drawback of our work is the added computational cost of the second forward pass during training, especially in contrast to inference-time only schemes, e.g., Wang et al. (2025a). However, the empirical results demonstrate that this trade-off of train-time compute is well worth the gains achieved on downstream evaluations.

Future Directions In follow up work, we plan to explore the disentangling of the corrector and unmasking models via weight untying or with completely separate neural network backbones for each model. Additionally, while we present a performant sampling algorithm, the ability to correct mistakes opens up the design space to more sophisticated schemes of jointly using corrector and unmasking steps, which we leave to future work to explore.

Impact Statement

This paper presents work whose goal is to advance the field of machine learning. Our work holds the promise for positive impact by accelerating inference and improving quality of language models. While, our method is also subject to the dangers of misuse present in language modeling, especially in the application to biological sequences, given the limited scale of models that we explore, the experiments described in this work do not pose any significant risks.

References

Arriola, M., Gokaslan, A., Chiu, J. T., Yang, Z., Qi, Z., Han, J., Sahoo, S. S., and Kuleshov, V. Block diffusion: Interpolating between autoregressive and diffusion language models. *arXiv preprint arXiv:2503.09573*, 2025.

Austin, J., Johnson, D. D., Ho, J., Tarlow, D., and Van Den Berg, R. Structured denoising diffusion models in discrete state-spaces. *Advances in Neural Information Processing Systems*, 34:17981–17993, 2021a.

Austin, J., Odena, A., Nye, M., Bosma, M., Michalewski, H., Dohan, D., Jiang, E., Cai, C., Terry, M., Le, Q., et al. Program synthesis with large language models. *arXiv preprint arXiv:2108.07732*, 2021b.

Ben-Hamu, H., Gat, I., Severo, D., Nolte, N., and Karrer, B. Accelerated sampling from masked diffusion models via entropy bounded unmasking. *arXiv preprint arXiv:2505.24857*, 2025.

Bercovich, A., Ailon, N., Anisimov, V., Asida, T., Assaf, N., Dabbah, M., Galil, I., Geifman, A., Geifman, Y., Golan, I., et al. Extending puzzle for mixture-of-experts reasoning models with application to gpt-oss acceleration. *arXiv preprint arXiv:2602.11937*, 2026.

Bickerton, G. R., Paolini, G. V., Besnard, J., Muresan, S., and Hopkins, A. L. Quantifying the chemical beauty of drugs. *Nature chemistry*, 4(2):90–98, 2012.

Bie, T., Cao, M., Chen, K., Du, L., Gong, M., Gong, Z., Gu, Y., Hu, J., Huang, Z., Lan, Z., et al. Llada2. 0: Scaling up diffusion language models to 100b. *arXiv preprint arXiv:2512.15745*, 2025.

Bie, T., Cao, M., Cao, X., Chen, B., Chen, F., Chen, K., Du, L., Feng, D., Feng, H., Gong, M., et al. Llada2. 1: Speeding up text diffusion via token editing. *arXiv preprint arXiv:2602.08676*, 2026.

Campbell, A., Benton, J., De Bortoli, V., Rainforth, T., Deligiannidis, G., and Doucet, A. A continuous time framework for discrete denoising models. *Advances in Neural Information Processing Systems*, 35:28266–28279, 2022.

Chen, M., Tworek, J., Jun, H., Yuan, Q., Pinto, H. P. D. O., Kaplan, J., Edwards, H., Burda, Y., Joseph, N., Brockman, G., et al. Evaluating large language models trained on code. *arXiv preprint arXiv:2107.03374*, 2021.

Chen, T., Zhang, R., and Hinton, G. Analog bits: Generating discrete data using diffusion models with self-conditioning. *arXiv preprint arXiv:2208.04202*, 2022.

Cobbe, K., Kosaraju, V., Bavarian, M., Chen, M., Jun, H., Kaiser, L., Plappert, M., Tworek, J., Hilton, J., Nakano, R., et al. Training verifiers to solve math word problems. *arXiv preprint arXiv:2110.14168*, 2021.

Dhariwal, P. and Nichol, A. Diffusion models beat gans on image synthesis. *Advances in neural information processing systems*, 34:8780–8794, 2021.

Dieleman, S., Sartran, L., Roshannai, A., Savinov, N., Ganin, Y., Richemond, P. H., Doucet, A., Strudel, R., Dyer, C., Durkan, C., et al. Continuous diffusion for categorical data. *arXiv preprint arXiv:2211.15089*, 2022.

Falcon, W. and The PyTorch Lightning team. PyTorch Lightning, March 2019. URL <https://github.com/Lightning-AI/lightning>.

Gao, L., Tow, J., Abbasi, B., Biderman, S., Black, S., DiPofi, A., Foster, C., Golding, L., Hsu, J., Le Noac’h, A., Li, H., McDonnell, K., Muennighoff, N., Ociepa, C., Phang, J., Reynolds, L., Schoelkopf, H., Skowron, A., Sutawika, L., Tang, E., Thite, A., Wang, B., Wang, K., and Zou, A. A framework for few-shot language model evaluation, 12 2023. URL <https://zenodo.org/records/10256836>.

Gat, I., Remez, T., Shaul, N., Kreuk, F., Chen, R. T., Synnaeve, G., Adi, Y., and Lipman, Y. Discrete flow matching. *arXiv preprint arXiv:2407.15595*, 2024.

Gokaslan, A. and Cohen, V. Openwebtext corpus. <http://SkyLion007.github.io/OpenWebTextCorpus>, 2019.

Grattafiori, A., Dubey, A., Jauhri, A., Pandey, A., Kadian, A., Al-Dahle, A., Letman, A., Mathur, A., Schelten, A., Vaughan, A., et al. The llama 3 herd of models. *arXiv preprint arXiv:2407.21783*, 2024.

Harris, C. R., Millman, K. J., van der Walt, S. J., Gommers, R., Virtanen, P., Cournapeau, D., Wieser, E., Taylor, J., Berg, S., Smith, N. J., Kern, R., Picus, M., Hoyer, S., van Kerkwijk, M. H., Brett, M., Haldane, A., del Río, J. F., Wiebe, M., Peterson, P., Gérard-Marchant, P., Sheppard, K., Reddy, T., Weckesser, W., Abbasi, H., Gohlke, C., and Oliphant, T. E. Array programming with NumPy. *Nature*, 585(7825):357–362, September 2020. doi: 10.1038/s41586-020-2649-2. URL <https://doi.org/10.1038/s41586-020-2649-2>.

- 495 Hendrycks, D., Burns, C., Kadavath, S., Arora, A., Basart,
496 S., Tang, E., Song, D., and Steinhardt, J. Measuring math-
497 ematical problem solving with the math dataset. *arXiv*
498 *preprint arXiv:2103.03874*, 2021.
- 499
500 Ho, J., Jain, A., and Abbeel, P. Denoising diffusion proba-
501 bilistic models. *Advances in neural information process-*
502 *ing systems*, 33:6840–6851, 2020.
- 503
504 Huang, Z., Wang, Y., Chen, Z., and Qi, G.-J. Don’t settle too
505 early: Self-reflective remasking for diffusion language
506 models. *arXiv preprint arXiv:2509.23653*, 2025.
- 507
508 Hunter, J. D. Matplotlib: A 2d graphics environment. *Com-*
509 *puting in Science & Engineering*, 9(3):90–95, 2007. doi:
510 10.1109/MCSE.2007.55.
- 511
512 Kim, J., Kim, S., Lee, T., Pan, D. Z., Kim, H., Kakade, S.,
513 and Chen, S. Fine-tuning masked diffusion for provable
514 self-correction. *arXiv preprint arXiv:2510.01384*, 2025a.
- 515
516 Kim, J., Shah, K., Kontonis, V., Kakade, S., and Chen,
517 S. Train for the worst, plan for the best: Understand-
518 ing token ordering in masked diffusions. *arXiv preprint*
519 *arXiv:2502.06768*, 2025b.
- 520
521 Kim, S. H., Hong, S., Jung, H., Park, Y., and Yun, S.-
522 Y. Klass: Kl-guided fast inference in masked diffusion
523 models. *arXiv preprint arXiv:2511.05664*, 2025c.
- 524
525 Kingma, D. P. Adam: A method for stochastic optimization.
526 *arXiv preprint arXiv:1412.6980*, 2014.
- 527
528 Kingma, D. P. and Welling, M. Auto-encoding variational
529 bayes. *arXiv preprint arXiv:1312.6114*, 2013.
- 530
531 Kuleshov, V. Fast algorithms for sparse principal component
532 analysis based on rayleigh quotient iteration. In *Interna-*
533 *tional Conference on Machine Learning*, pp. 1418–1425.
534 PMLR, 2013.
- 535
536 Landrum, G. et al. Rdkit: A software suite for cheminforma-
537 tics, computational chemistry, and predictive modeling.
538 *Greg Landrum*, 8(31.10):5281, 2013.
- 539
540 Lezama, J., Salimans, T., Jiang, L., Chang, H., Ho, J., and
541 Essa, I. Discrete predictor-corrector diffusion models for
542 image synthesis. In *The Eleventh International Confer-*
543 *ence on Learning Representations*, 2023.
- 544
545 Li, X., Thackstun, J., Gulrajani, I., Liang, P. S., and
546 Hashimoto, T. B. Diffusion-lm improves controllable
547 text generation. *Advances in Neural Information Process-*
548 *ing Systems*, 35:4328–4343, 2022.
- 549
550 Liu, L., Huang, B., Liu, X., Yin, B., and Zhao, T. Teach dif-
551 fusion language models to learn from their own mistakes.
552 *arXiv preprint arXiv:2601.06428*, 2026.
- 553
554 Lou, A., Meng, C., and Ermon, S. Discrete diffusion mod-
555 eling by estimating the ratios of the data distribution. In
556 *Forty-first International Conference on Machine Learn-*
557 *ing*, 2024.
- 558
559 Meshchaninov, V., Shibaev, E., Makoian, A., Klimov, I.,
560 Sheshenya, D., Malinin, A., Balagansky, N., Gavrilov, D.,
561 Alanov, A., and Vetrov, D. Guided star-shaped masked
562 diffusion. *arXiv preprint arXiv:2510.08369*, 2025.
- 563
564 Nie, S., Zhu, F., You, Z., Zhang, X., Ou, J., Hu, J., Zhou, J.,
565 Lin, Y., Wen, J.-R., and Li, C. Large language diffusion
566 models. *arXiv preprint arXiv:2502.09992*, 2025.
- 567
568 OpenAI. gpt-oss-120b & gpt-oss-20b model card, 2025.
569 URL <https://arxiv.org/abs/2508.10925>.
- 570
571 Ou, J., Nie, S., Xue, K., Zhu, F., Sun, J., Li, Z., and Li,
572 C. Your absorbing discrete diffusion secretly models the
573 conditional distributions of clean data. *arXiv preprint*
574 *arXiv:2406.03736*, 2024.
- 575
576 pandas development team, T. pandas-dev/pandas: Pan-
577 das, February 2020. URL <https://doi.org/10.5281/zenodo.3509134>.
- 578
579 Paszke, A., Gross, S., Massa, F., Lerer, A., Bradbury, J.,
580 Chanan, G., Killeen, T., Lin, Z., Gimelshein, N., Antiga,
581 L., Desmaison, A., Kopf, A., Yang, E., DeVito, Z., Rai-
582 son, M., Tejani, A., Chilamkurthy, S., Steiner, B., Fang,
583 L., Bai, J., and Chintala, S. PyTorch: An Imperative Style,
584 High-Performance Deep Learning Library. In Wallach,
585 H., Larochelle, H., Beygelzimer, A., d’Alché Buc, F.,
586 Fox, E., and Garnett, R. (eds.), *Advances in Neural Infor-*
587 *mation Processing Systems 32*, pp. 8024–8035. Curran
588 Associates, Inc., 2019.
- 589
590 Peebles, W. and Xie, S. Scalable diffusion models with
591 transformers. In *Proceedings of the IEEE/CVF Internat-*
592 *ional Conference on Computer Vision*, pp. 4195–4205,
593 2023.
- 594
595 Peng, F. Z., Bezemek, Z., Patel, S., Rector-Brooks, J., Yao,
596 S., Bose, A. J., Tong, A., and Chatterjee, P. Path planning
597 for masked diffusion model sampling. *arXiv preprint*
598 *arXiv:2502.03540*, 2025.
- 599
600 Pillutla, K., Swayamdipta, S., Zellers, R., Thackstun, J.,
601 Welleck, S., Choi, Y., and Harchaoui, Z. Mauve: Mea-
602 suring the gap between neural text and human text using
603 divergence frontiers. *Advances in Neural Information*
604 *Processing Systems*, 34:4816–4828, 2021.
- 605
606 Radford, A., Wu, J., Child, R., Luan, D., Amodei, D.,
607 Sutskever, I., et al. Language models are unsupervised
608 multitask learners. *OpenAI blog*, 1(8):9, 2019.

- Ramakrishnan, R., Dral, P. O., Rupp, M., and Von Lilienfeld, O. A. Quantum chemistry structures and properties of 134 kilo molecules. *Scientific data*, 1(1):1–7, 2014.
- Ruddigkeit, L., Van Deursen, R., Blum, L. C., and Reymond, J.-L. Enumeration of 166 billion organic small molecules in the chemical universe database gdb-17. *Journal of chemical information and modeling*, 52(11):2864–2875, 2012.
- Sahoo, S. S., Arriola, M., Gokaslan, A., Marroquin, E. M., Rush, A. M., Schiff, Y., Chiu, J. T., and Kuleshov, V. Simple and effective masked diffusion language models. In *The Thirty-eighth Annual Conference on Neural Information Processing Systems*, 2024a. URL <https://openreview.net/forum?id=L4uaAR4ArM>.
- Sahoo, S. S., Gokaslan, A., Sa, C. D., and Kuleshov, V. Diffusion models with learned adaptive noise. In *The Thirty-eighth Annual Conference on Neural Information Processing Systems*, 2024b. URL <https://openreview.net/forum?id=loMa99A4p8>.
- Savinov, N., Chung, J., Binkowski, M., Elsen, E., and Oord, A. v. d. Step-unrolled denoising autoencoders for text generation. *arXiv preprint arXiv:2112.06749*, 2021.
- Schiff, Y., Sahoo, S. S., Phung, H., Wang, G., Boshar, S., Dalla-torre, H., de Almeida, B. P., Rush, A., Pierrot, T., and Kuleshov, V. Simple guidance mechanisms for discrete diffusion models. *arXiv preprint arXiv:2412.10193*, 2024.
- Schwaller, P., Laino, T., Gaudin, T., Bolgar, P., Hunter, C. A., Bekas, C., and Lee, A. A. Molecular transformer: A model for uncertainty-calibrated chemical reaction prediction. *ACS central science*, 5(9):1572–1583, 2019.
- Shi, J., Han, K., Wang, Z., Doucet, A., and Titsias, M. K. Simplified and generalized masked diffusion for discrete data. *arXiv preprint arXiv:2406.04329*, 2024.
- Sohl-Dickstein, J., Weiss, E., Maheswaranathan, N., and Ganguli, S. Deep unsupervised learning using nonequilibrium thermodynamics. In *International conference on machine learning*, pp. 2256–2265. PMLR, 2015.
- Song, Y. and Ermon, S. Generative modeling by estimating gradients of the data distribution. *Advances in neural information processing systems*, 32, 2019.
- Song, Y., Sohl-Dickstein, J., Kingma, D. P., Kumar, A., Ermon, S., and Poole, B. Score-based generative modeling through stochastic differential equations. *arXiv preprint arXiv:2011.13456*, 2020.
- Sun, H., Yu, L., Dai, B., Schuurmans, D., and Dai, H. Score-based continuous-time discrete diffusion models. *arXiv preprint arXiv:2211.16750*, 2022.
- von Rütte, D., Fluri, J., Ding, Y., Orvieto, A., Schölkopf, B., and Hofmann, T. Generalized interpolating discrete diffusion. *arXiv preprint arXiv:2503.04482*, 2025.
- Wang, G., Schiff, Y., Sahoo, S. S., and Kuleshov, V. Re-masking discrete diffusion models with inference-time scaling. *arXiv preprint arXiv:2503.00307*, 2025a.
- Wang, G., Schiff, Y., Turok, G., and Kuleshov, V. d2: Improved techniques for training reasoning diffusion language models. *arXiv preprint arXiv:2509.21474*, 2025b.
- Wang, Y., Schiff, Y., Gokaslan, A., Pan, W., Wang, F., De Sa, C., and Kuleshov, V. InfoDiffusion: Representation learning using information maximizing diffusion models. In Krause, A., Brunskill, E., Cho, K., Engelhardt, B., Sabato, S., and Scarlett, J. (eds.), *Proceedings of the 40th International Conference on Machine Learning*, volume 202 of *Proceedings of Machine Learning Research*, pp. 36336–36354. PMLR, 23–29 Jul 2023. URL <https://proceedings.mlr.press/v202/wang23ah.html>.
- Waskom, M. L. seaborn: statistical data visualization. *Journal of Open Source Software*, 6(60):3021, 2021. doi: 10.21105/joss.03021. URL <https://doi.org/10.21105/joss.03021>.
- Weininger, D. Smiles, a chemical language and information system. 1. introduction to methodology and encoding rules. *Journal of chemical information and computer sciences*, 28(1):31–36, 1988.
- Wolf, T., Debut, L., Sanh, V., Chaumond, J., Delangue, C., Moi, A., Cistac, P., Rault, T., Louf, R., Funtowicz, M., et al. Huggingface’s transformers: State-of-the-art natural language processing. *arXiv preprint arXiv:1910.03771*, 2019.
- Wu, C., Zhang, H., Xue, S., Liu, Z., Diao, S., Zhu, L., Luo, P., Han, S., and Xie, E. Fast-dllm: Training-free acceleration of diffusion llm by enabling kv cache and parallel decoding. *arXiv preprint arXiv:2505.22618*, 2025.
- Yadan, O. Hydra - a framework for elegantly configuring complex applications. Github, 2019. URL <https://github.com/facebookresearch/hydra>.
- Ye, J., Xie, Z., Zheng, L., Gao, J., Wu, Z., Jiang, X., Li, Z., and Kong, L. Dream 7b, 2025. URL <https://hkunlp.github.io/blog/2025/dream>.
- Zhao, L., Ding, X., Yu, L., and Akoglu, L. Improving and unifying discrete&continuous-time discrete denoising diffusion. *arXiv preprint arXiv:2402.03701*, 2024a.
- Zhao, Y., Shi, J., Mackey, L., and Linderman, S. Informed correctors for discrete diffusion models. *arXiv preprint arXiv:2407.21243*, 2024b.

605 Zheng, K., Chen, Y., Mao, H., Liu, M.-Y., Zhu, J., and
606 Zhang, Q. Masked diffusion models are secretly time-
607 agnostic masked models and exploit inaccurate categori-
608 cal sampling. *arXiv preprint arXiv:2409.02908*, 2024.

609 Zhu, F., Wang, R., Nie, S., Zhang, X., Wu, C., Hu, J., Zhou,
610 J., Chen, J., Lin, Y., Wen, J.-R., et al. Llada 1.5: Variance-
611 reduced preference optimization for large language diffu-
612 sion models. *arXiv preprint arXiv:2505.19223*, 2025.

613
614
615
616
617
618
619
620
621
622
623
624
625
626
627
628
629
630
631
632
633
634
635
636
637
638
639
640
641
642
643
644
645
646
647
648
649
650
651
652
653
654
655
656
657
658
659

A. Deriving *ProSeCo* from MCMC Predictor-Corrector

We now show how we can derive the corrector loss term \mathcal{L}^C from the objective in (3) by leveraging formulations from predictor-corrector sampling for continuous-time Markov chains (Campbell et al., 2022). In particular, we start from the perspective that sampling errors are a byproduct of the fact that the posteriors of the learned reverse process do not align with those from predefined corruption process $p_\theta(\mathbf{z}_s | \mathbf{z}_t) \neq q(\mathbf{z}_s | \mathbf{z}_t)$. This issue arises because of two reasons, 1) the model may not fully capture the exact marginals of each token position, and 2) the inherent parameterization of our reverse process as factorized independently across the sequence length dimension does not account for cross-token dependencies (Ben-Hamu et al., 2025). These deviations compound along a generation path and ultimately lead to marginals that are significantly divergent $p_\theta(\mathbf{z}_t) \neq q(\mathbf{z}_t)$. In score-matching generative modeling for continuous data (Song et al., 2020), this mismatch can be mitigated by Langevin Monte Carlo Markov chain (MCMC) iterations. Unfortunately in the discrete data setting, we do not have access to a continuous score function that drives the predictor-corrector sampler proposed in Song et al. (2020).

Crucially, Campbell et al. (2022) demonstrate that for discrete data we can also apply corrector steps and produce a MCMC that yields $q(\mathbf{z}_t)$ as its stationary distribution. Interleaving corrector MCMC steps with predictor (unmasking) ones enables us to recover from deviations before proceeding along the generation trajectory. While Campbell et al. (2022) observe better sample quality with their proposed ‘forward-backward’ corrector scheme, follow up works (Lezama et al., 2023; Zhao et al., 2024a) note that this methodology can be further improved by learning the reverse transition kernel for the corrector MCMC, leading to more ‘informed’ corrector steps.

At a high level, our derivation below proceeds as follows. We first propose a corrector sampling chain. We then prove that if the corrector distribution satisfies a given functional form then we will achieve our goal of having the samples from the MCMC corrector step $\sim q(\mathbf{z}_t^{1:L})$. Finally, we enforce this condition by minimizing a divergence between the corrector distribution induced by our model and the desired form. This training recovers the corrector loss proposed in Section 3.

Corrector MCMC In the vein of learned predictor-corrector works (Lezama et al., 2023), we define an MCMC corrector step by the following chain:

$$\begin{aligned} 1) & \text{ Sample } \mathbf{y}_t^{1:L} \sim p_\theta(\mathbf{y}_t^{1:L} | \mathbf{z}_t^{1:L}), \\ 2) & \text{ Sample } \hat{\mathbf{x}}^{1:L} \sim p_\phi(\hat{\mathbf{x}}^{1:L} | \mathbf{y}_t^{1:L}), \\ 3) & \text{ Sample } \hat{\mathbf{z}}_t^{1:L} \sim q(\hat{\mathbf{z}}_t^{1:L} | \hat{\mathbf{x}}^{1:L}), \end{aligned} \quad (6)$$

where $p_\theta(\mathbf{y}_t^{1:L} | \mathbf{z}_t^{1:L}) = \prod_{\ell=1}^L \text{Cat}(\mathbf{y}_t^\ell; \mathbf{x}_\theta^\ell(\mathbf{z}_t^{1:L}))$ is the distribution defined by parallel decoding from the output of our denoising network \mathbf{x}_θ and $q(\hat{\mathbf{z}}_t^{1:L} | \hat{\mathbf{x}}^{1:L})$ follows the factorized masked diffusion forward process, introduced in Section 2. Additionally, p_ϕ represents a corrector model with parameters ϕ .

Intuitively the sampling chain above represents the following correction mechanism: 1) we sample from the denoising model’s prediction given the current latent variable, $\mathbf{y}_t^{1:L} \sim p_\theta(\mathbf{y}_t^{1:L} | \mathbf{z}_t^{1:L})$, then 2) given this sample, the corrector predicts the clean data distribution, and we sample from this prediction, $\hat{\mathbf{x}}^{1:L} \sim p_\phi(\hat{\mathbf{x}}^{1:L} | \mathbf{y}_t^{1:L})$, and finally 3) we re-noise the sample from the corrector output according to the predefined noising process, $\hat{\mathbf{z}}_t^{1:L} \sim q(\hat{\mathbf{z}}_t^{1:L} | \hat{\mathbf{x}}^{1:L})$. The goal of this chain is that the re-noised latent variable $\hat{\mathbf{z}}_t^{1:L}$ more closely resembles draws from the true distribution $q(\mathbf{z}_t^{1:L})$.

Detailed Balance Condition We now describe a condition on p_ϕ that will achieve this goal.

Proposition A.1. *The following form will ensure the detailed balanced condition, with $q(\mathbf{z}_t^{1:L})$ as the stationary distribution:*

$$p_\phi(\mathbf{x}^{1:L} | \mathbf{y}_t^{1:L})q(\mathbf{z}_t^{1:L} | \mathbf{x}^{1:L}) = \frac{p_\theta(\mathbf{y}_t^{1:L} | \mathbf{z}_t^{1:L})q(\mathbf{z}_t^{1:L} | \mathbf{x}^{1:L})q_{data}(\mathbf{x}^{1:L})}{Z(\mathbf{y}_t^{1:L})}, \quad (7)$$

where $Z(\mathbf{y}_t^{1:L})$ is a normalization constant representing the marginal probability of $\mathbf{y}_t^{1:L}$.

Proof. We prove this using a similar argument to that presented in Lezama et al. (2023). Specifically, let $R(\hat{\mathbf{z}}_t^{1:L} | \mathbf{z}_t^{1:L})$ denote the transition kernel defined by the sampling chain in (6), then

$$q(\mathbf{z}_t^{1:L})R(\hat{\mathbf{z}}_t^{1:L} | \mathbf{z}_t^{1:L}) = q(\mathbf{z}_t^{1:L}) \sum_{\mathbf{y}_t^{1:L}} \sum_{\mathbf{x}^{1:L}} p_\phi(\mathbf{x}^{1:L} | \mathbf{y}_t^{1:L})q(\hat{\mathbf{z}}_t^{1:L} | \mathbf{x}^{1:L})p_\theta(\mathbf{y}_t^{1:L} | \mathbf{z}_t^{1:L}) \quad \{From (6)\}$$

$$\begin{aligned}
 &= q(\mathbf{z}_t^{1:L}) \sum_{\mathbf{y}_t^{1:L}} \sum_{\mathbf{x}^{1:L}} \left(\frac{p_\theta(\mathbf{y}_t^{1:L} | \hat{\mathbf{z}}_t^{1:L}) q(\hat{\mathbf{z}}_t^{1:L} | \mathbf{x}^{1:L}) q_{\text{data}}(\mathbf{x}^{1:L})}{Z(\mathbf{y}_t^{1:L})} \right) p_\theta(\mathbf{y}_t^{1:L} | \mathbf{z}_t^{1:L}) && \{From (7)\} \\
 &= q(\hat{\mathbf{z}}_t^{1:L}) \sum_{\mathbf{y}_t^{1:L}} \left(\frac{p_\theta(\mathbf{y}_t^{1:L} | \hat{\mathbf{z}}_t^{1:L}) q(\hat{\mathbf{z}}_t^{1:L})}{Z(\mathbf{y}_t^{1:L})} \right) p_\theta(\mathbf{y}_t^{1:L} | \mathbf{z}_t^{1:L}) && \{Marginalize \mathbf{x}\} \\
 &= q(\hat{\mathbf{z}}_t^{1:L}) \sum_{\mathbf{y}_t^{1:L}} \left(\frac{p_\theta(\mathbf{y}_t^{1:L} | \mathbf{z}_t^{1:L}) q(\mathbf{z}_t^{1:L})}{Z(\mathbf{y}_t^{1:L})} \right) p_\theta(\mathbf{y}_t^{1:L} | \hat{\mathbf{z}}_t^{1:L}) && \{Note 'role change' of \mathbf{z}_t \& \hat{\mathbf{z}}_t\} \\
 &= q(\hat{\mathbf{z}}_t^{1:L}) \sum_{\mathbf{y}_t^{1:L}} \sum_{\mathbf{x}^{1:L}} \left(\frac{p_\theta(\mathbf{y}_t^{1:L} | \mathbf{z}_t^{1:L}) q(\mathbf{z}_t^{1:L} | \mathbf{x}^{1:L}) q_{\text{data}}(\mathbf{x}^{1:L})}{Z(\mathbf{y}_t^{1:L})} \right) p_\theta(\mathbf{y}_t^{1:L} | \hat{\mathbf{z}}_t^{1:L}) \\
 &= q(\hat{\mathbf{z}}_t^{1:L}) \sum_{\mathbf{y}_t^{1:L}} \sum_{\mathbf{x}^{1:L}} p_\phi(\mathbf{x}^{1:L} | \mathbf{y}_t^{1:L}) q(\mathbf{z}_t^{1:L} | \mathbf{x}^{1:L}) p_\theta(\mathbf{y}_t^{1:L} | \hat{\mathbf{z}}_t^{1:L}) && \{From (7)\} \\
 &= q(\hat{\mathbf{z}}_t^{1:L}) R(\mathbf{z}_t^{1:L} | \hat{\mathbf{z}}_t^{1:L}). && \{From (6)\}
 \end{aligned}$$

□

Maximum Likelihood Corrector Training Having shown that the condition in (7) is sufficient for achieving the desired limiting distribution $q(\mathbf{z}_t^{1:L})$ for the corrector MCMC, we can cast the corrector training as ensuring that $p_\phi(\mathbf{x}^{1:L} | \mathbf{y}_t^{1:L}) q(\mathbf{z}_t^{1:L} | \mathbf{x}^{1:L}) \propto p_\theta(\mathbf{y}_t^{1:L} | \mathbf{z}_t^{1:L}) q(\mathbf{z}_t^{1:L} | \mathbf{x}^{1:L}) q_{\text{data}}(\mathbf{x}^{1:L})$ (Lezama et al., 2023). We can achieve this by minimizing the following objective:

$$\begin{aligned}
 &D_{\text{KL}}[p_\theta(\mathbf{y}_t^{1:L} | \mathbf{z}_t^{1:L}) q(\mathbf{z}_t^{1:L} | \mathbf{x}^{1:L}) q_{\text{data}}(\mathbf{x}^{1:L}) || p_\phi(\mathbf{x}^{1:L} | \mathbf{y}_t^{1:L}) q(\mathbf{z}_t^{1:L} | \mathbf{x}^{1:L}) Z(\mathbf{y}_t^{1:L})] \\
 &= -\mathbb{E}_{\mathbf{x}^{1:L} \sim q_{\text{data}}(\mathbf{x}^{1:L})} \mathbb{E}_{\mathbf{z}_t^{1:L} \sim q(\mathbf{z}_t^{1:L} | \mathbf{x}^{1:L})} \mathbb{E}_{\mathbf{y}_t^{1:L} \sim p_\theta(\mathbf{y}_t^{1:L} | \mathbf{z}_t^{1:L})} [\log p_\phi(\mathbf{x}^{1:L} | \mathbf{y}_t^{1:L})] + C,
 \end{aligned} \tag{8}$$

where C represents factors that do not depend on ϕ . Minimizing this objective ensures that the distribution over latents $\mathbf{z}_t^{1:L}$ induced by the corrector steps aligns with the true marginal distributions.

Parameterizing the Corrector Model Finally, similar to the denoising model, we parameterize the corrector to be independent across the sequence length dimension given its inputs, as follows:

$$p_\phi(\mathbf{x}^{1:L} | \mathbf{y}_t^{1:L}) = \prod_{\ell=1}^L p_\phi(\mathbf{x}^\ell | \mathbf{y}_t^{1:L}), \quad \text{with } p_\phi(\mathbf{x}^\ell | \mathbf{y}_t^{1:L}) = \text{Cat}(\mathbf{x}^\ell; \mathbf{x}_\phi^\ell(\mathbf{y}_t^{1:L})), \tag{9}$$

where $\mathbf{x}_\phi^\ell(\mathbf{z}_t^{1:L}) \in \Delta^V$ for all $\ell \in \{1, \dots, L\}$ is the output of a corrector model network. This independent factorization for the corrector model enables us to maintain parallel generation.

Using this factorized parameterization and replacing the sampling of $\mathbf{y}_t^{1:L}$ with the transformation $\pi \circ \mathbf{x}_\theta^{1:L}$ defined in Section 3.1 recovers the \mathcal{L}^C corrector loss term from the objective in (3):

$$\mathcal{L}^C = \log \langle \mathbf{x}_\phi^\ell(\mathbf{y}_t^{1:L}), \mathbf{x}^\ell \rangle.$$

B. Sampling with *ProSeCo* Semi-Autoregressively

In Algorithm 4, we present a modified version of our sampling method from Algorithm 2, which accommodates the block autoregressive decoding proposed in Arriola et al. (2025) and adopted by LLaDA (Nie et al., 2025). Given that we applied block AR decoding to the LLaDA models, the implementation provided in Algorithm 4 assumes full bidirectional attention is applied across the entire sequence at every forward pass, as in LLaDA, and is not written to support key-value (KV) caching. However, this algorithm can be easily adapted to support efficient KV caching proposed in Arriola et al. (2025).

Notably, for *ProSeCo* with semi-AR decoding, at every correction iteration, clean tokens in the current block and all previously decoded blocks can be adapted.

Algorithm 4 *ProSeCo* Sampling Block Autoregressive

```

770 # Assumes full bidirectional attention without KV-caching, as in LLaDA.
771 # Differences to standard MDM with block AR decoding highlighted in brown.
772 1: Input: Model  $\mathbf{x}_\theta$ , length  $L$ , block size  $B$ , unmasking steps  $T$ , noise schedule  $\alpha_t$ , self-correction budget (per step)  $S$ , corrector
773 frequency  $\omega$ .
774 2: Initialize  $\mathbf{z}_{t(T)}^{1:L} \leftarrow \mathbf{m}^{1:L}$ 
775 3: for  $b = 1$  to  $(L/B)$  do
776 4:   for  $i = T$  to  $1$  do
777 5:     logits  $\leftarrow \mathbf{x}_\theta(\mathbf{z}_i^{1:L})$ 
778 6:     if  $(T - i + 1) \bmod \omega == 0$  then
779 7:        $\mathbf{z}_i^{1:L}, \text{logits} \leftarrow \text{corrector}(\mathbf{x}_\theta, \mathbf{z}_i^{1:L}, S)$ 
780 8:     end if
781 9:     logits $^\ell \leftarrow -\infty, \forall \ell \in [1, (b-1) \cdot B] \cup [b \cdot B + 1, L]$ 
782 10:     $\mathbf{z}_{t(i-1)}^{1:L} \leftarrow \text{sample\_posterior}(\text{logits}, \mathbf{z}_i^{1:L}, \alpha_{t(i)})$ 
783 11:  end for
784 12:   $\mathbf{z}_{t(0)}^\ell \leftarrow \text{sample}(\mathbf{x}_\theta^\ell(\mathbf{z}_{t(0)}^{1:L})), \forall \ell \in [1 + (b-1) \cdot B, b \cdot B]$ 
785 13:   $\mathbf{z}_{t(T)}^{1:L} \leftarrow \mathbf{z}_{t(0)}^{1:L}$ 
786 14: end for
787 15: Return  $\mathbf{z}_{t(0)}^{1:L}$ 

```

C. Additional Experimental Details

C.1. Math & Code Benchmarks

Dataset Our SFT dataset is a modified version of the Llama-Nemotron-Post-Training dataset (Bercovich et al., 2026), comprising approximately 32 million samples across four core domains: mathematical reasoning, coding, science, and instruction following. The distribution is heavily skewed toward math (66.84%) and coding (30.62%), with smaller allocations for science (2.15%), instruction following (0.17%), chat (0.12%), and safety (0.10%). All target outputs were generated using GPT-OSS (OpenAI, 2025) in high-reasoning mode.

Training Hyperparameters We fine-tuned the LLaDA-Base 8B model for ~ 400 B tokens, which amounts to 3 epochs of training on our SFT dataset. We train with a batch size of 1024. For learning rate we linearly warm-up for 1000 gradient steps until a maximum learning rate of $2.5e^{-5}$. After this peak, we apply cosine decay until a minimum learning rate of $2.5e^{-7}$. We use the ADAM-w optimizer (Kingma, 2014) with beta parameters (0.9, 0.999). Finally, during training it is common to set a `min_t > 0` value which biases the sampling of timesteps away from uniform over the unit interval, by shifting all samples to be in the range $[\text{min_t}, 1]$. For example, in works such as Sahoo et al. (2024b), this value is set to $1e^{-3}$. For our SFT experiments, we found that biasing towards heavier masking during training led to improved performance, hence we set `min_t` to $1e^{-1}$.

Compute resources We fine-tuned both our model and the baseline using 256 NVIDIA B200 GPUs, and conducted all evaluation runs on 8 NVIDIA H100 GPUs.

Evaluation For evaluation, we rely on the Nemo Skills library. We evaluate all models with batch size 1. This is to mitigate varying padding lengths based on prompt size variation and to enable effective use of early-stopping whenever the `[EOS]` token is generated. All evaluated models use a maximum generation length of 1024.

We evaluate 4 benchmarks: HumanEval (Chen et al., 2021) and MBPP (Austin et al., 2021b), GSM8K (Cobbe et al., 2021) and MATH (Hendrycks et al., 2021). We use 0-shot evaluation for each benchmark.

For LLaDA models, we use a semi-AR decoding scheme (Arriola et al., 2025), as in Nie et al. (2025), with default block size of 32.

Prompts and Evaluation Templates Below, we detail the templates used for evaluating models in Table 1. These prompts were used for all models, except the off-the-shelf LLaDA-Base model. For HumanEval and MBPP the placeholder `{question}` is replaced by the prompt from the benchmark dataset. Similarly, for GSM8K and MATH, the placeholder `{problem}` is replaced by the prompt from the benchmark dataset. Additionally, we use the default chat templates from the Nemo Skills library.

Note that for LLaDA-Base, we do not provide any additional prompt text, we only use the benchmark question as given.

	Here is a problem for which you need to generate/complete code: {question}
HumanEval / MBPP Prompt:	Please continue to complete the function with python programming language. You are not allowed to modify the given code and do the completion only. The solution should be in the following format: ``python # Your code here ``
GSM8K / MATH Prompt:	Solve the following math problem. Show your step-by-step reasoning, then provide the final answer inside \boxed{ } {problem}

Sampling Hyperparameters When evaluating *ProSeCo* models, we explore different configurations of unmasking and corrector budgets. In Table 3, we detail the sampling hyperparameters used to generate the best performing results for *ProSeCo* Max reported in Table 1 and Figure 3; see Appendix D.3 for more details. Note that T represents a maximum unmasking budget, since we apply early stopping on the [EOS] token. Additionally, S represents a maximum corrector budget per correction loop, because we break the loop iterations if a corrector sequence does not change between rounds.

For Figure 4 (and Figure 6, below), we use the Fast configuration, applying a corrector loop every 4 unmasking steps, with a maximum of 2 corrector steps per loop.

Table 3. Sampling hyperparameters for results attained with *ProSeCo* and reported in Figure 3.

	HumanEval	MBPP	GSM8K	MATH
<i>Baseline (Vanilla SFT)</i>				
Accuracy (%)	58.54	56.88	88.86	46.60
Average NFEs	247.8	290.3	214.2	259.4
Generation length	1024	1024	1024	1024
Block length	32	32	32	32
Demasking Tokens/Step	1	1	1	1
<i>ProSeCo Max</i>				
Accuracy (%)	72.56	69.31	92.19	55.06
Average NFEs	499.2	818.3	342.5	747.5
Generation length	1024	1024	1024	1024
Block length	32	32	32	32
Demasking Tokens/Step	1	1	1	1
Corrector frequency ω	2	1	2	2
Maximum corrector steps per loop S	4	8	1	8
<i>ProSeCo Balanced</i>				
Accuracy (%)	70.12	66.93	91.28	54.36
Average NFEs	213.9	218.7	228.7	321.2
Generation length	1024	1024	1024	1024
Block length	32	32	32	32
Demasking Tokens/Step	4	4	4	4
Corrector frequency ω	1	1	1	1
Maximum corrector steps per loop S	8	8	8	8
<i>ProSeCo Fast</i>				
Accuracy (%)	60.98	62.70	90.90	49.56
Average NFEs	61.4	110.9	119.5	81.2
Generation length	1024	1024	1024	1024
Block length	32	32	32	32
Demasking Tokens/Step	8	4	4	8
Corrector frequency ω	2	2	2	2
Maximum corrector steps per loop S	4	4	4	4

Baselines For all prior work results, other than ReMeDi (Huang et al., 2025), we use open-source weights and evaluate using with batch size 1, maximum generation length of 1024, and early stopping on the [EOS] token. For ReMeDi Instruct, we

report values from [Huang et al. \(2025\)](#), as we were unable to reproduce or improve upon their results using the open-source model provided.

All model evaluations, other than for the off-the-shelf LLaDA-Base model, were performed using the Nemo Skills library, using default chat templates from this library and the prompt templates described above. For LLaDA-Base, since the Nemo Skills repository injects chat templates by default, we evaluate using the lm-eval-harness repository.

For ReMDM, we follow the algorithm proposed by [Wang et al. \(2025a\)](#) for applying this method to LLaDA. Namely, for each block of 32 tokens, once 28 tokens have been generated, we enable a ReMDM loop, where for 32 iterations we remask 2 tokens that had the lowest confidence at the time at which they were decoded and unmask 2 tokens based on their confidence. Hence, at the end of the ReMDM loop, there are still 28 unmasked and 4 masked tokens, at which point we finish generating using the standard LLaDA confidence-based sampling.

C.2. Guided Molecule Design

For this experiment, we follow the setup detailed in [Schiff et al. \(2024\)](#).

Dataset We train on the QM9 dataset ([Ramakrishnan et al., 2014](#); [Ruddigkeit et al., 2012](#)), which consists of $\sim 133k$ molecules represented as SMILES strings ([Weininger, 1988](#)). We use the RDKit library ([Landrum et al., 2013](#)) to add the ring count and drug likeness (QED; ([Bickerton et al., 2012](#))) annotations. The dataset was tokenized using a regular expression tokenizer ([Schwaller et al., 2019](#)). We use sequence length of $L = 32$, with right-padding.

For each property, we generate binary labels that indicate whether a sample is below or above the 90th percentile of training samples. For discrete classifier-free-guidance ([Schiff et al., 2024](#)), we train with this label for conditional models, and randomly ‘drop it out’ 10 percent of the time by replacing it with a ‘masked’ label to simulate unconditional modeling.

Hyperparameters Hyperparameters follow [Schiff et al. \(2024\)](#). Namely, we use a DiT-style ([Peebles & Xie, 2023](#)) backbone with 92.4M parameters. Models were trained with a batch size 2048, and we perform 25k gradient updates. We use a maximum learning rate of $3e^{-4}$ that we linearly warm-up to for 1000 steps. After this peak we apply cosine decay until a minimum learning rate of $3e^{-6}$. We use the ADAM-w with beta parameters (0.9, 0.999).

Of note, when training *PraSeCo* models for ring count, we found it beneficial to eliminate the ‘copy over’ parameterization of the denoising network \mathbf{x}_θ proposed in [Sahoo et al. \(2024a\)](#). That is, we do not enforce that \mathbf{x}_θ simply copy over any token positions $\mathbf{z}_i^t \neq m$. For training models for the QED property, we maintained this copy-over parameterization.

Compute Resources We trained our model on 8 A5000 GPUs.

Evaluation We generate 1024 samples from our model using various unmasking budgets T and guidance temperature γ . Of note, when applying the corrector model forward passes, we only use the conditional model, i.e., $\gamma = 1$.

We use the RDKit library to parse generated samples. Of the valid strings (those that can be parsed) we retain unique samples that are not found in the original QM9 dataset (novel). We then use RDKit to measure the property of interest for these novel samples.

Sampling Hyperparameters For both ring count and QED maximization we use $\omega = T/2$ for corrector loop frequency and $S = T/16$ for steps per loop. Evaluation was performed with an exponential moving average (EMA) checkpoint. During training we used an EMA decay factor of 0.9999.

Baselines Values for AR, UDLM, MDLM, and ReMDM were taken from [Wang et al. \(2025a\)](#).

For ReMeDi ([Huang et al., 2025](#)) and GStar ([Meshchaninov et al., 2025](#)), we re-implement these methods and train them on the QM9 dataset. Both of these methods entail training a classifier that predicts incorrect tokens to remask.

For ReMeDi, we jointly train their ‘‘Unmasking Policy Stream’’ (UPS) alongside an MDLM model. We use the ‘‘dual stream’’ architecture recommended by [Huang et al. \(2025\)](#), with 4 DiT layers for the UPS, connected to the main backbone at layers 0, 3, 7, and 10. We set the UPS loss weight at $\lambda_{\text{UPS}} = 0.3$. For the proportion of unmasked tokens that get flipped to random tokens we use $\rho_{t,\text{incorrect}} = 0.1$. Finally, as ReMeDi was not originally proposed within the context of classifier-free guidance, to have a fair comparison, we perform a hyperparameter sweep for this model over the following parameters: whether to apply the classifier-free guidance (CFG) to only the ‘‘Token Prediction Stream’’ (i.e., the MDLM output) or also to the UPS and whether to use sampling or greedy-max selection when choosing which tokens to remask. We found best results when applying CFG to both streams and when using proportional sampling, not greedy-max selection, for remasking positions.

In GStar, the error prediction head is trained with a frozen diffusion backbone model, hence we use the pre-trained MDLM from Wang et al. (2025a) and freeze its weights. The error prediction head consists of a `LayerNorm` and linear projection from the final hidden token representations of the frozen backbone. We employ the ‘‘GStar+’’ sampling algorithm and for fair comparison we perform a sweep over the following parameters: whether to apply the CFG to only the MDLM output or also to the remasking prediction head, whether to use Gumbel top- k or greedy top- k selection during remasking, the temperature for both the MDLM (sweep over $\{0.7, 1.0, 1.3\}$) and remasking head output (sweep over $\{2, 4, 8, 16\}$), and the remasking switch-on time (sweep over $\{0.1, 0.2, 0.3, 0.4\}$). For the ring count property, we found best results using Gumbel top- k , switch time 0.2, denoiser temperature 0.7, and prediction head temperature 16. For the QED property, we found best results using greedy top- k , switch time 0.4, and denoiser temperature 1.0.

C.3. Unconditional Text Generation

For this experiment, we follow the setup described in Sahoo et al. (2024a).

Dataset We train models on the OpenWebText (OWT; (Gokaslan & Cohen, 2019)) dataset. We tokenized using the `gpt-2` (Radford et al., 2019) tokenizer and created sequences of $L = 1024$ tokens by wrapping samples and separating them with an `[EOS]` token. We also place an `[EOS]` token at the beginning and end of each sequence.

Hyperparameters As in Sahoo et al. (2024a), we use a DiT backbone with 170M parameters. We used a batch size of 512 and applied 1M gradient updates. We use a constant learning rate of $3e^{-4}$ that we linearly warm-up to for 2500 steps. We use the ADAM-w optimizer with beta parameters (0.9, 0.999). As described in Appendix C.1, we use a `min_t` value of $1e^{-1}$, when training *ProSeCo* models on OWT.

For training *ProSeCo* in this setting, we found it beneficial to eliminate the ‘copy over’ parameterization of the denoising network \mathbf{x}_θ .

Compute Resources We trained our model on 32 H100 GPUs.

Evaluation We follow the evaluation protocol from Wang et al. (2025a). Specifically, we generate 5000 samples and compute the MAUVE metric (Pillutla et al., 2021), generative perplexity under the `gpt2-large` model, and entropy of generated tokens.

Modified Training Objective For this experiment, we use a slightly modified objective relative to that presented in Algorithm 1. Specifically, we adjust the self-correction term \mathcal{L}^{SC} so that gradients for tokens which the original denoiser model incorrectly predicts are steeper. To accomplish this, we replace the self-correction loss term from Algorithm 1 with the following:

$$\tilde{\mathcal{L}}^{SC}(\theta) := \frac{\alpha_t}{1 - \alpha_t} \sum_{\ell=1}^L \delta_{\mathbf{y}_t^\ell, \mathbf{x}^\ell} \langle \mathbf{x}_\theta^\ell(\mathbf{y}_t^{1:L}), \mathbf{x}^\ell \rangle + (1 - \delta_{\mathbf{y}_t^\ell, \mathbf{x}^\ell}) \log \langle \mathbf{x}_\theta^\ell(\mathbf{y}_t^{1:L}), \mathbf{x}^\ell \rangle. \quad (10)$$

The modified loss term in (10) has the desirable property that token positions where the original denoiser model predicts a mistake, i.e. $\delta_{\mathbf{y}_t^\ell, \mathbf{x}^\ell} = 0$, are prioritized. This is accomplished by the fact that the gradient for the standard cross-entropy loss used for these token positions is steeper than that for positions where the denoising model is ‘already correct’, i.e., $\delta_{\mathbf{y}_t^\ell, \mathbf{x}^\ell} = 1$, where the loss is taken without the logarithm.

Modified Sampling Procedure Additionally, for the samples presented in Table 2, we use a slightly modified sampling procedure. Rather than simply using `arg max` decoding at every token position for the `sample` sub-routine in the `corrector` function in Algorithm 2, at each corrector step, we sort all positions by the confidence of the `arg max` token. Then, for the top- k positions, we use the `arg max` token, and for the remaining positions, we leave them unchanged. We use $k = 100$ and found that this procedure better encouraged sample diversity and improved MAUVE scores. In Algorithm 5, we detail the top- k sampling sub-routine that we use for corrector sampling in the OWT experiments.

Sampling Hyperparameters For *ProSeCo*, we match the inference budget of baseline results by using number of unmasking steps equal to $T/4$ per column, performing a corrector loop at every iteration, $\omega = 1$, and applying 3 corrector steps per loop, $S = 3$. We use $k = 100$ as the top- k parameter for Algorithm 5. Evaluation was performed with an EMA checkpoint. During training we used an EMA decay factor of 0.9999.

Baselines Values for the baseline models were taken from Wang et al. (2025a), except for PRISM results which were taken from Kim et al. (2025a). For PRISM, results correspond to the ‘PRISM-loop’ method presented in Table 3 of Kim et al.

Algorithm 5 Corrector sample sub-routine used in OWT experiments

```

1: Input: Corrector model input  $\mathbf{y}_t^{1:L}$ , corrector model output corrector_logits, parameter  $k$ 
2:  $\hat{\mathbf{y}}^{1:L} \leftarrow \arg \max(\text{corrector\_logits})$ 
   # 'gather' is an API that returns values of its first input at the indices specified by
   # its second input, see for example torch.gather (with dim=-1)
3:  $\text{confidence\_scores} \leftarrow \text{gather}(\text{corrector\_logits}, \hat{\mathbf{y}}^{1:L})$ 
4: for  $\ell = 1$  to  $L$  do
5:   if  $\hat{\mathbf{y}}^\ell \neq \mathbf{y}_t^\ell$  then
6:      $\text{confidence\_scores}^\ell \leftarrow -\infty$ 
7:   end if
8: end for
   # 'top_k' is an API that returns the top k argument positions for its first input
9:  $\text{top\_k\_indices} \leftarrow \text{top\_k}(\text{confidence\_scores}, k)$ 
10: for  $\ell = 1$  to  $L$  do
11:   if  $\ell \in \text{top\_k\_indices}$  then
12:      $\mathbf{y}_t^\ell \leftarrow \hat{\mathbf{y}}^\ell$ 
13:   else
14:      $\mathbf{y}_t^\ell \leftarrow \mathbf{y}_t^\ell$ 
15:   end if
16: end for
17: Return  $\mathbf{y}_t^{1:L}$ 

```

(2025a).

For GIDD (von Rütte et al., 2025), we use the $p_u = 0.2$ open-source checkpoint provided by the authors. Since this model was trained on sequence length of $L = 512$, in contrast to the other comparisons and our model which use $L = 1024$, we evaluate the GIDD model with $L = 512$. We use temperature parameter equal to 0.1, and we allow an equal number of unmasking and self-correction steps. Since the self-correction algorithm proposed in GIDD can terminate prior to exhausting the full budget, in Table 4 we denote the GIDD configurations used to match the GIDD results to the various T budgets in Table 2. Note that for certain T , we err on the side of allowing the GIDD model to exceed the total budget T .

Table 4. Parameters used for GIDD (von Rütte et al., 2025) unmasking and self-correction budgets corresponding to the results in Table 2.

$T =$	Unmasking steps	Maximum Self Correction Steps	Avg. NFEs
128	64	64	123.9
256	128	128	212.6
512	512	512	601.3
1024	1024	1024	1114.2

D. Additional Experimental Results

D.1. Quality-Efficiency Tradeoffs

In Table 5, we compare the baseline method to the *ProSeCo* Max, Balanced, and Fast configurations and report throughput (in tokens per second, TPS) as well as the accuracy and efficiency gains. In Figure 6, we also repeat our Pareto frontier results from Figure 4, with throughput reported.

D.2. Ablation: Robustness to Corrector Parameters

In Figure 7, we demonstrate that our model, which underwent SFT with *ProSeCo* training, is highly robust to the choice of the corrector sampling parameters, i.e., the frequency of corrector loops ω and number of corrector steps per loop S . We look at various levels of unmasking parallelism, ranging from fully sequential at tokens/step = 1 to tokens/step = 8, and evaluate our model with $\omega \in \{1, 2, 4, 8\}$ and $S \in \{1, 2, 4, 8\}$. In particular, we see that at every level of decoding parallelism, our model can beat the best performing Baseline SFT results for all choices of ω and S .

A few additional observations from Figure 7, in the first two rows, corresponding to ‘fast sampling’ regimes, in order to match or exceed the best baseline accuracy, which is attained with tokens/step = 1, we require more frequent corrector

Table 5. Quality vs. Efficiency Metrics. We report Accuracy (%), Average Number of Function Evaluations (NFEs), and Throughput (Tokens/Second). Best accuracy gain and efficiency results are **bolded**. Improvements over the baseline are highlighted in **green**.

	HumanEval	MBPP	GSM8K	MATH
<i>Baseline (Vanilla SFT)</i>				
Accuracy	58.54	56.88	88.86	46.60
Avg. NFEs	247.8	290.3	214.2	259.4
Tokens/Second	123.14	131.04	148.92	153.15
<i>ProSeCo Max</i>				
Accuracy (+ gain)	72.56 (+14.0)	69.31 (+12.4)	92.19 (+3.3)	55.06 (+8.5)
Avg. NFEs (\times speedup)	499.2 (0.50 \times)	818.3 (0.35 \times)	342.5 (0.63 \times)	747.5 (0.35 \times)
Tokens/Second (\times speedup)	59.66 (0.48 \times)	37.48 (0.29 \times)	103.83 (0.70 \times)	61.38 (0.40 \times)
<i>ProSeCo Balanced</i>				
Accuracy (+ gain)	70.12 (+11.6)	66.93 (+10.1)	91.28 (+2.4)	54.36 (+7.8)
Avg. NFEs (\times speedup)	213.9 (1.16 \times)	218.7 (1.33 \times)	228.7 (0.94 \times)	321.2 (0.81 \times)
Tokens/Second (\times speedup)	137.07 (1.11 \times)	131.15 (1.00 \times)	158.33 (1.06 \times)	141.94 (0.93 \times)
<i>ProSeCo Fast</i>				
Accuracy (+ gain)	60.98 (+2.4)	62.70 (+5.8)	90.90 (+2.0)	49.56 (+3.0)
Avg. NFEs (\times speedup)	61.4 (4.04\times)	110.9 (2.62\times)	119.5 (1.79\times)	81.2 (3.19\times)
Tokens/Second (\times speedup)	455.01 (3.70\times)	251.92 (1.92\times)	304.33 (2.04\times)	512.27 (3.34\times)

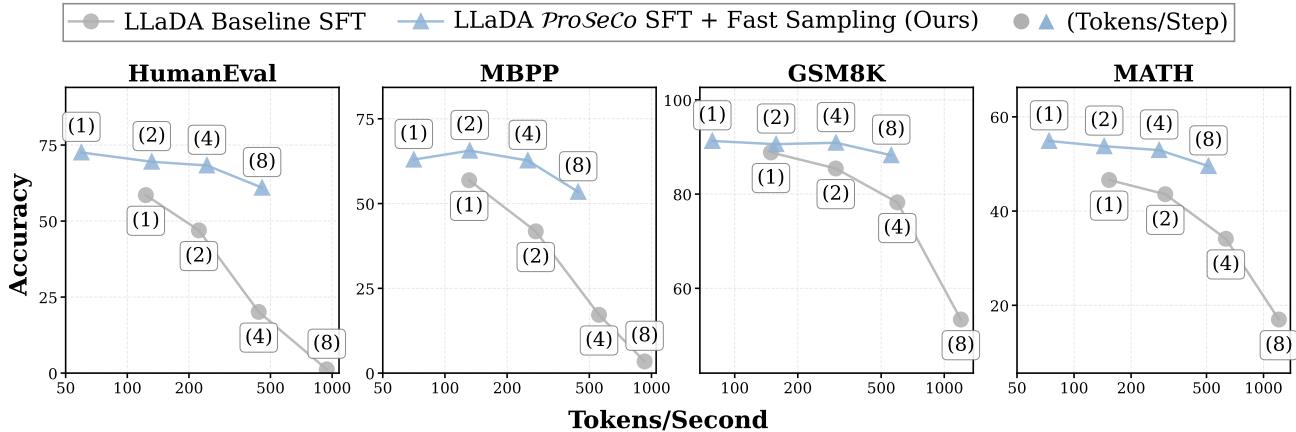


Figure 6. Pareto frontier analysis with throughput (tokens per second, TPS) reported.

loops $\omega \in \{1, 2\}$. In these settings we can drastically improve efficiency relative to the baseline model. In this fast sampling regime, we also see a general trend that, for a fixed corrector budget (i.e., $S \cdot L/\omega$), more frequent but shorter correction loops are typically more effective. Additionally, when unmasking sampling increases to tokens/step $\in \{1, 2\}$, we find the expected trend that scaling both frequency of correction loops and number of steps per loop leads almost uniformly to improved sample quality, at the cost of additional NFEs.

D.3. Selecting the Max, Balanced, and Fast Points

From the hyperparameter sweep described in Appendix D.2, we selected representative points as *ProSeCo* Max, Balanced, and Fast. The chosen parameters for each of these are detailed in Table 3. For the Max configuration, we selected the best overall *ProSeCo* performance from the sweep performed in Figure 7. For the Fast configuration, we selected points from parallel generation of either tokens/step = 4 or tokens/step = 8 where we attain better accuracy than the best baseline performance, which uses tokens/step = 1. For the Balanced configuration, we anchor tokens/step = 4, and select a configuration that pushes the boundary to the north-west across all benchmarks.

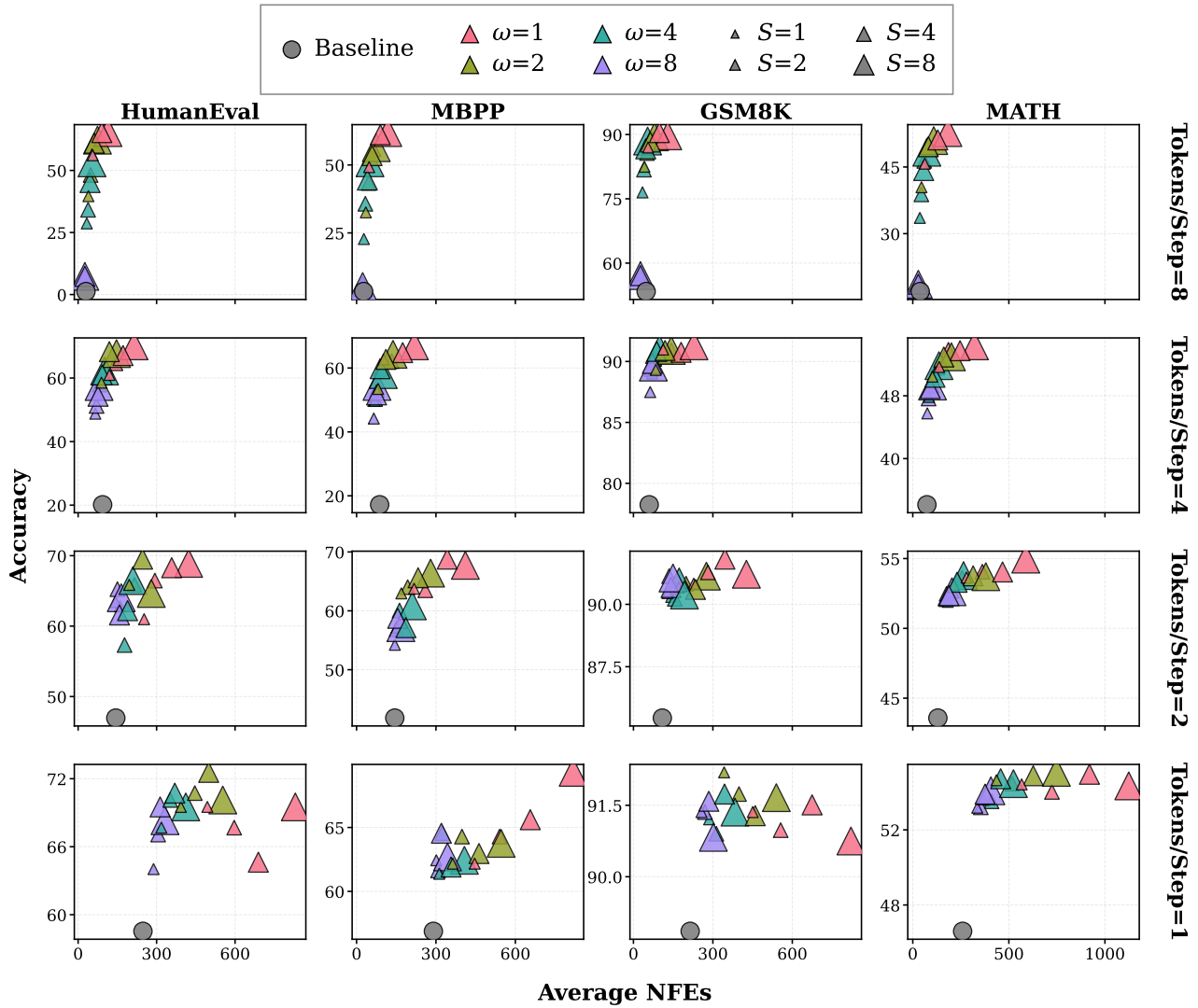


Figure 7. Ablation: Performance across various configurations of corrector steps. Frequency $\omega \in \{1, 2, 4, 8\}$ (denoted by color) and $S \in \{1, 2, 4, 8\}$ (denoted by marker size).

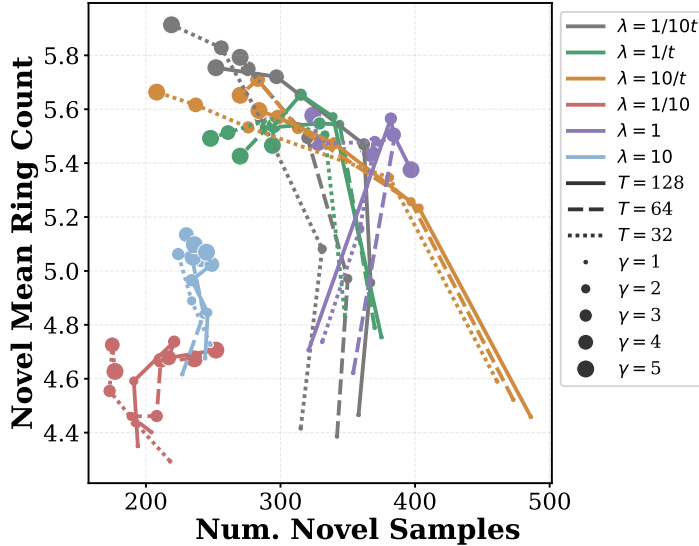


Figure 8. Ablation: Selecting self-correction loss weight λ_t . We retrain the discrete classifier model for maximizing ring count with various λ_t values.

D.4. Ablation: Self-correction Sampling with Standard MDM

In Table 6, we demonstrate the importance of *ProSeCo* training, by comparing self-correction sampling applied to a model with standard MDM SFT vs. one with *ProSeCo* loss and Algorithm 1. These results underscore the importance of training a model to self-correct. With standard MDM training, the model does not learn to produce meaningful predictions at already unmasked token locations. Our method unlocks this ability, and therefore benefits from the self-correction sampling algorithm.

Table 6. Ablation: Applying self-correction sampling to models trained with standard MDM loss leads to worse performance, underscoring the importance of the *ProSeCo* framework. Pass@1 accuracy (%) performance is reported.

Training + Sampling	HumanEval	MBPP	GSM8K	MATH
Vanilla SFT + Standard MDM	58.54	56.88	88.86	46.60
Vanilla SFT + <i>ProSeCo</i> Balanced	1.83	1.85	60.42	27.06
<i>ProSeCo</i> SFT + <i>ProSeCo</i> Balanced	72.56	69.31	92.19	55.06

D.5. Ablation: Selecting λ_t

Below we present the ablation on the self-correction loss term weight. We run training for discrete classifier guidance on the ring count property with fixed $\lambda \in \{0.1, 1, 10\}$ and a time-varying weighted $\lambda_t \in \{0.1 \cdot \frac{\alpha_t}{(1-\alpha_t)}, 1 \cdot \frac{\alpha_t}{(1-\alpha_t)}, 10 \cdot \frac{\alpha_t}{(1-\alpha_t)}\}$. We report results in Figure 8. We find that using the $\frac{\alpha_t}{1-\alpha_t}$ weighting consistently improves results. Furthermore, our model is robust to different scalings of this time-dependent weighting.

D.6. Error Bars for Table 2

In Table 7, we report mean \pm standard error from four random seeds used during sampling for our model’s results on unconditional generation (Table 2).

E. Generated Samples

E.1. LLaDA *ProSeCo* SFT Samples

In Figures 9 and 10, we present sample generations for the HumanEval and GSM8K datasets, respectively, using the maximum accuracy configuration for each benchmark (see Table 3).

Table 7. Mean \pm standard error for OWT unconditional generation metrics for *ProSeCo*.

$T =$	MAUVE (\uparrow)	Gen. PPL (\downarrow)	Entropy (\uparrow)
128	0.311 ± 0.006	23.045 ± 0.031	5.452 ± 0.002
256	0.572 ± 0.006	16.52 ± 0.014	5.376 ± 0.005
512	0.622 ± 0.005	13.196 ± 0.031	5.293 ± 0.001
1024	0.592 ± 0.006	10.92 ± 0.014	5.221 ± 0.005

E.2. *ProSeCo* Unconditional Generation Samples

In Figure 11, we present a sample generated from the *ProSeCo* model trained on OWT. We use total sample budget of $T = 256$, which consists of 64 unmasking steps, a corrector loop every $\omega = 1$ step, and $S = 3$ corrector steps per loop.

F. Assets

In Table 8, we list the corresponding licenses for datasets used in this work.

Table 8. Datasets and corresponding licenses.

Dataset	Licence
GSM8K (Cobbe et al., 2021)	MIT
HumanEval (Chen et al., 2021)	MIT
Llama-Nemotron: Efficient Reasoning Models (Bercovich et al., 2026)	CC BY 4.0
MBPP (Austin et al., 2021b)	MIT
MinveraMath (Hendrycks et al., 2021)	MIT
OpenWebText (Gokaslan & Cohen, 2019)	Creative Commons CC0 license ("no rights reserved")
QM9 (Ramakrishnan et al., 2014; Ruddigkeit et al., 2012)	N/A

In Table 9, we list the corresponding licenses for software packages used in this work.

Table 9. Software and corresponding licenses.

Library	License
HuggingFace (Wolf et al., 2019)	Apache 2.0
Hydra (Yadan, 2019)	MIT
Fast-DLLM (Wu et al., 2025)	Apache 2.0
Language Model Evaluation Harness (Gao et al., 2023)	MIT
Matplotlib (Hunter, 2007)	Matplotlib license
Mauve (Pillutla et al., 2021)	GNU General Public License, Version 3
MDLM (Sahoo et al., 2024a)	Apache 2.0
Nemo Skills	Apache 2.0
NumPy (Harris et al., 2020)	NumPy license
OmegaConf	BSD 3-Clause
Pandas (pandas development team, 2020)	BSD 3-Clause "New" or "Revised"
PyTorch (Paszke et al., 2019)	BSD-3 Clause
PyTorch Lightning (Falcon & The PyTorch Lightning team, 2019)	Apache 2.0
RDKit (Landrum et al., 2013)	BSD 3-Clause "New" or "Revised"
Seaborn (Waskom, 2021)	BSD 3-Clause "New" or "Revised"
TorchMetrics	Apache 2.0
UDLM (Schiff et al., 2024)	Apache 2.0

G. Impact Statement

Our paper is intended as a contribution to the machine learning community. Our work holds the promise for positive impact by accelerating inference and improving quality of language models. While, our method is also subject to the dangers of misuse present in language modeling, especially in the application to biological sequences, given the limited scale of models that we explore, the experiments described in this work do not pose any significant risks.

1265 **H. LLM Usage Disclosure**

1266 Large Language Models (LLMs) were used to format and edit this manuscript and for formatting figures. Additionally,
1267 integrated LLMs in the code editing software used while developing this work were used for auto-complete suggestions and
1268 in debugging.
1269

1270 LLMs were **not** used for the core development of our methodology, derivation of key results, nor the programming of our
1271 main code and experiments.
1272

1273

1274

1275

1276

1277

1278

1279

1280

1281

1282

1283

1284

1285

1286

1287

1288

1289

1290

1291

1292

1293

1294

1295

1296

1297

1298

1299

1300

1301

1302

1303

1304

1305

1306

1307

1308

1309

1310

1311

1312

1313

1314

1315

1316

1317

1318

1319

HumanEval Sample**Prompt shown to the model**

Here is a problem for which you need to generate/complete code:

```
def make_a_pile(n):
    """
    Given a positive integer n, you have to make a pile of n levels of stones.
    The first level has n stones.
    The number of stones in the next level is:
        - the next odd number if n is odd.
        - the next even number if n is even.
    Return the number of stones in each level in a list, where element at index
    i represents the number of stones in the level (i+1).

    Examples:
    >>> make_a_pile(3)
    [3, 5, 7]
    """
```

Please continue to complete the function with python programming language. You are not allowed to modify the given code and do the completion only.

The solution should be in the following format:

```
```python
Your code here
```
```

Model output

```
```python
def make_a_pile(n):
 """
 Given a positive integer n, you have to make a pile of n levels of stones.
 The first level has n stones.
 The number of stones in the next level is:
 - the next odd number if n is odd.
 - the next even number if n is even.
 Return the number of stones in each level in a list, where element at index
 i represents the number of stones in the level (i+1).

 Examples:
 >>> make_a_pile(3)
 [3, 5, 7]
 """
 pile = []
 for i in range(1, n + 1):
 if i % 2 == 1: # odd level -> next odd number
 pile.append(2 * i - 1)
 else: # even level -> next even number
 pile.append(2 * i)
 return pile
```
```

Figure 9. Example of *ProSeCo*'s generated response on the HumanEval dataset using the max accuracy configuration (see Table 3).

1375
1376
1377
1378
1379
1380
1381
1382
1383
1384
1385
1386
1387
1388
1389
1390
1391
1392
1393
1394
1395
1396
1397
1398
1399
1400
1401
1402
1403
1404
1405
1406
1407
1408
1409
1410
1411
1412
1413
1414
1415
1416
1417
1418
1419
1420
1421
1422
1423
1424
1425
1426
1427
1428
1429

GSM8K Sample; Expected answer: 6

Prompt shown to the model

Solve the following math problem. Show your step-by-step reasoning, then provide the final answer inside `\boxed{}`.

Solo has to read 4 pages from his Science textbook, 20 pages from his Social Studies textbook, 7 pages from his History textbook and 8 pages from his Geography textbook. Solo read 15 pages on Monday. If he has 4 more days to complete all his reading, how many pages does he need to read, on average, in one day?

Model output

Step-by-step reasoning

1. **Total pages to be read**

$$4 + 20 + 7 + 8 = 39 \text{ pages}$$
 2. **Pages already read**

$$15 \text{ pages on Monday}$$
 3. **Pages left to read**

$$39 - 15 = 24 \text{ pages}$$
 4. **Number of days left**

$$4 \text{ more days}$$
 5. **Average pages per day**

$$\frac{24 \text{ pages}}{4 \text{ days}} = 6 \text{ pages per day}$$
- `\boxed{6}`

Figure 10. Example of *ProSeCo*'s generated response on the GSM8K dataset using the max accuracy configuration (see Table 3).

OWT Generated Sample

“**lendoftextl** campaigns trying to figure out how to raise money for a ballot measure America’s political dailies have not adopted an information-delivery strategy. Teich’s most recent foray was, according to its spokeswoman, a brand new social media campaign that it took a break from advertising the previous year, and launched on its website. Both stem from a tradition of public-sector philanthropy, and position the company as a public utility whose funding is in no way tied to government spending or health care. We have reached out to Teich for more information, and so far have received no response.

But Teich has all but abandoned its information delivery strategy—or at least when it comes to what it calls its “frontiers.”

While its Indiegogo campaign has been focused on social issues, much of it has centered on public health and safety initiatives in an effort to reduce the number of traffic deaths, make driving less dangerous, reduce dependence on oil and to improve the health of people in a developing country. Its

budgeted nearly \$60 million in fiscal year 2016, according to Teich Institute, a nonprofit that tracks Teich’s spending.

Back in 2014, the year it launched, the company calculated how much it could spend on new software, or new nurses, or programs that focus on technology. It spends a big chunk of that money on budgeting—but there are different approaches to health care spending. For instance, some decide what kind of money they spend; others decide how much money they spend on a particular service. So how much Teich spends depends on the investment.

You’ve heard of this about health-care. The Obama health-care bill seemed to cost \$200 billion—but neither the White House nor the administration said anything about how much it cost. Teich has put its total at \$20 billion.

“The big question for me is not just whether Teich decides to spend too much, but whether TARP looks at spending too much,” says Erin McAllister, executive director of the Teich Public Policy Institute. That calculation helps explain how much Teich spent to fight the opioid epidemic here in Washington D.C., she says, though she says she doesn’t know just how much that money went to a particular cause.

Students, for instance, know how to gamble. “They probably knew what they were going to spend,” she says. “What surprises me is that people don’t know when they buy something that is going to have a bigger impact on an institution than an investment.”

Subscribe to Smart Money’s Smart Money app—you can download it here.

In some cases, Teich says it didn’t know how much of its money was spent, so it didn’t disclose how much the company spent. That likely happened in 2010 and 2012, for “from an investment perspective, you’re basically going the other way to buy something that’s going to have a bigger impact than an investment,” McAllister says. “You may see something that has less impact than investment, and you may see something that has more impact and less impact than investment.”

In New York City—where Teich’s Indiegogo campaign spent nearly \$50 million in fiscal year 2016—it managed to convince advocacy groups to spend the bulk of its money on television ads. The company and its partners estimated that the campaign would finance net \$2 million in television ads over the next 12 months. In other cities, similar things happen year after year, McAllister says.

So much depends on the investment. The public-sector infrastructure bought by Teich remains relatively small. Its advertising strategies have changed little over the years, and they continue to attract big-name attention.

Of its most recent investments in public health, Ken Farrell, a lawyer with the President’s Office, agrees that Teich has designed previous advertising campaigns that have largely paid off. But McAllister says the payoff could be quite big, depending on how much the company spends.

The company’s sticker price has been criticized by elected officials, environmental groups and those who ignore the fossil fuel industry at their peril. But its spending on public health initiatives has been relatively steady—it’s spent almost \$650 million since 2010. Neither Trump or his administration has really pushed for new regulations despite concerns about their potential benefits. And experts aren’t totally convinced that new taxes will improve public health—especially because of the already unacceptably high tolls and highway tolls in the United States. Tax advocates will argue that new taxes will be good for everyone—but are skeptical.

“It’s compelling,” Stan Diem, a political science professor at Wesleyan University says. “But there is no evidence that it is**lendoftextl**”

Figure 11. Generated sample from *ProSeCo* trained on OWT, with a total budget of $T = 256$: 64 unmasking steps, corrector frequency $\omega = 1$ and $S = 3$ steps per loop.